LOS ALAMOS SCIENTIFIC LABORATORY

OF THE UNIVERSITY OF CALIFORNIA

LOS ALAMOS, NEW MEXICO

CONTRACT W-7405-ENG.36 WITH THE
U.S. ATOMIC ENERGY COMMISSION

[redacted] UNCLASSIFIED

UNCLASSIFIED

LOS ALAMOS SCIENTIFIC LABORATORY
of the
UNIVERSITY OF CALIFORNIA

Report written:
June 1955

DO NOT CIRCULATE
Retention Copy

LAMS-1935
C.2
This document consists of 89 pages
No. [redacted] of 20 copies, Series A.

UNCLASSIFIED

A COMPILATION OF SPECTROSCOPIC OBSERVATIONS OF AIR AROUND ATOMIC BOMB EXPLOSIONS

Report Prepared By
Hugh E. DeWitt

Work Done By

NRL Optics Division
H. S. Stewart
L. F. Drummeter, Jr.
J. A. Curcio
C. H. Duncan
J. H. Campbell

LASL Liaison
W. E. Ogle
L. B. Seely, Jr.
Herman Hoerlin

LASL Consultant
G. H. Dieke (Johns Hopkins University)

[redacted]

UNCLASSIFIED

UNCLASSIFIED

Report distributed: SEP 2 1955

LAMS-1935

Los Alamos Report Library	1-14
Western Development Division, ARDC	15-20

ABSTRACT

This report presents a description of the spectra observed in atomic bomb explosions and a summary of data from recent series of tests on the spectroscopy of disturbed air around such explosions. A description of the stages of the explosion of a nominal bomb is given to aid understanding the observed spectra. The spectra of the first few milliseconds are primarily due to air and reaction products in air while the spectra of the much later period of the second maximum are due to absorption by the metallic constituents of the bomb in addition to air. Absorption by excited oxygen and such air reaction products as NO_2, HNO_2, O_3 and OH is discussed in detail. Some data on the time variation of the concentrations of these substances are given.

It is hoped that some of this information will be useful in estimating the amount of radiation from the hot air behind the shock front of a high velocity missile.

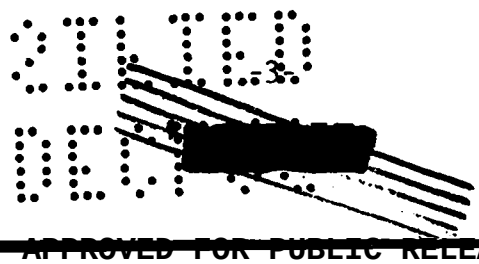

PREFACE

This report was written in order to make information about spectra available to various companies which are working on the ICBM Project.

The experimental work reported here was done by the Naval Research Laboratory under the direction and sponsorship of Los Alamos Scientific Laboratory. In various places verbatim quotations have been made from the reports of the members of the Naval Research Laboratory. Nearly all the figures of this report are taken directly from reports of the NRL, others are composite drawings based on NRL data. The theoretical analysis of the spectra again is quoted nearly verbatim from a report by G. H. Dieke.

Only a very small part of the present report is original work by Hugh DeWitt. His work mainly consisted of extracting from the NRL reports and from that of Dieke those parts which are relevant to the ICBM problem.

H. A. Bethe

CONTENTS

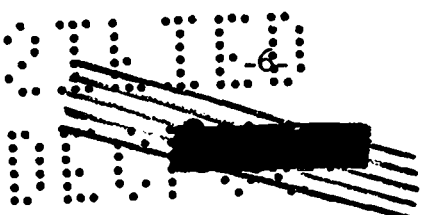

1. INTRODUCTION

The following report tries to summarize the available information on the spectroscopy of air in the neighborhood of atomic bomb explosions. This information comes mainly from several Los Alamos and Naval Research Laboratory reports dealing with spectrographic observations taken during bomb tests. It is hoped that some of this material may be useful in estimating the amount of radiation from the hot air behind the shock front surrounding the nose of a missile moving at Mach 15 to 25.

The condition of air disturbed by the shock wave and the radiation from a nuclear explosion differs somewhat from the air behind the shock front around a high velocity missile. In order to understand this difference and to understand the spectra observed from nuclear explosions, a description is given in the next section of the explosion of a nominal atomic bomb.

A nominal bomb is one releasing the energy equivalent of 20,000 tons of TNT. A "ton of TNT" is by definition 4.185×10^{16} ergs; hence the nominal bomb energy is 8.37×10^{20} ergs. All that is said about times and distances involved in the explosion of a nominal size bomb can be related to the same quantities for bombs of smaller or larger yields by means of scaling laws.

2. DESCRIPTION OF A NUCLEAR EXPLOSION

The most profound difference between a nuclear and a chemical explosion is that the former liberates its energy in a much smaller volume. In consequence the initial temperature is far higher, about a million degrees when a nuclear bomb bursts its case. This means that a significant fraction of the total energy, actually about one third, is released in the form of thermal radiation. This thermal radiation is intimately associated with the formation and development of the shock wave during the early stages of the explosion. It is also the light source for absorption spectra obtained during the two or three seconds that it lasts. The light observed from a distance is essentially black body radiation corresponding to temperatures between 2,000 and 10,000°K, but modified by the absorption due to normal air, reaction products in the air about the bomb, and bomb constituents.

2.1 Initial Stage of the Explosion: Radiation Expansion

During the first tenth of a millisecond or so the temperature is so high that radiation is the most rapid mechanism of energy transfer. Consequently a region of several meters radius about the bomb is heated to several hundred thousand degrees before it is set into motion by hydrodynamic effects. This is the period of "radiation expansion".

Radiation expansion occurs because the average mean free path of radiation at high temperatures is a strongly increasing function of

temperature, approximately T^3. At 1,000,000° the average mean free path (the Rosseland mean free path) is approximately one meter in air of normal density. A true shock wave cannot form immediately because the radiation front moves ahead so rapidly that a shock front would be completely smeared out. The volume of air and vaporized metal within the radiation front is brought quickly to the same uniform temperature throughout. As the radiation front expands, rapid cooling takes place, and the average mean free path of radiation decreases. At some fairly definite radius of about ten meters the radiation expansion comes to an end with the formation of an enormous shock wave because the velocity of the radiation front falls below the velocity of shock transmission. Temperature seems to play a unique role; it may be stated that an air shock will form when the temperature within the radiation front has dropped to approximately 300,000°K. Thereafter the shock front sweeps rapidly ahead of the radiation front and the behavior of the blast soon becomes independent of the radiation from behind the shock.

2.2 The Fireball and the Isothermal Core

At 1 msec after the explosion the observer will see a "ball of fire" with a radius of about 35 meters, and a surface temperature of perhaps 20,000°K. The term "ball of fire" refers to the total mass of air which is hot enough to radiate visible light. Inside the fireball there is a hotter inner core called the isothermal sphere. The material enclosed by this sphere is bounded by an internal radiation front. The

temperature inside is so hot that the core is transparent to its own radiation, and hence no thermal gradients can exist. Thus the sphere is isothermal in that it has the same temperature throughout, but of course this temperature decreases as the sphere expands.

The shock front defining the ball of fire moves ahead much faster than the internal radiation front and engulfs more air as it expands. The isothermal sphere also expands, but much more slowly than the shock front. Not much new material is engulfed by the internal radiation front.

Because of radiation transport the temperature at the shock front is smeared out so that there is no longer a discontinuity. The discontinuity of pressure is reduced. A rough theory has been developed to describe the effect of radiation on the shock front.[1] The temperature across the front is found to be:

$$T = T_s \left(1 - \frac{z}{z_o}\right)^{1/6}$$

where T_s is the shock temperature, z is the distance in front of the shock, and z_o is that distance in front of the shock at which the temperature becomes normal air temperature. The value of z_o varies as T_s^6; when R is 10 meters, which is about the distance where the shock front first forms, z_o is calculated to be 13 centimeters. Taylor and McCall[2] showed that this smearing out does not affect the shock velocity

[1] J. L. Magee and J. O. Hirschfelder, Thermal Radiation Phenomena, Chpt. 4, LA-1020, August 1947.

[2] G. I. Taylor and McCall, Durand's Aerodynamics, Vol. III (J. Springer, Berlin, 1936).

or pressure, but of course it does have a very profound effect on the radiation emitted by the shock wave.

For several milliseconds after the radiation expansion period of the explosion the ball of fire is bounded by a shock front at which the temperature increases by thousands of degrees. The shocked air behind the front absorbs radiation from the isothermal core and thus gets hotter deeper inside. At the internal radiation front the temperature rises to a hundred thousand degrees or so. During this time the surface of the fireball, the shock front, is assumed to radiate as a black body with a temperature corresponding to the shock temperature. In other words, the shock front is highly opaque, and very little radiation from the much hotter inner core gets outside the fireball.

2.3 Development of the Blast During the First 10 Msec

For a period of ten milliseconds or so after the air shock is formed the behavior or the blast is described fairly well by the theory of G. I. Taylor.[3] His theory starts with the assumption that a very large amount of energy is released instantaneously in a small volume. Radiation is neglected. The following similarity conditions are assumed behind the shock front:

pressure, $$\frac{p}{p_o} = R^{-3} f_1 \left(\frac{r}{R}\right)$$

[3] G. I. Taylor, Proc. Roy. Soc. London A201, 159 (1950).

density, $$\frac{\rho}{\rho_o} = \Psi\ (\frac{r}{R})$$

radial velocity, $$u = R^{-3/2}\, \Phi_1\ (\frac{r}{R})$$

where R is the radius of the shock front, p_o and ρ_o are the pressure and density of the undisturbed atmosphere, r is the radial coordinate, and the functions f_1, Ψ and Φ_1 are determined by integration of the hydrodynamic equations. For sufficiently large shock strengths, say $p_s/p_o \sim 5$, these similarity conditions can be matched to the Rankine-Hugoniot relations which must hold across the shock front. The boundary conditions on f_1, Ψ, and Φ_1 so obtained are the starting points for numerical integration.

Taylor obtains:

$$R = S(\gamma)\ (\frac{E}{\rho_o})^{1/5}\ t^{2/5}$$

$$\frac{dR}{dt} = \frac{2}{5}\, S(\gamma)\ (\frac{E}{\rho_o})^{1/5}\ t^{-3/5}$$

where E is the total energy of the blast and $S(\gamma)$ is a function of the specific heats determined by numerical integration. For the peak shock pressure and temperature Taylor's theory gives:

$$\frac{p_s}{p_o} = \frac{2\gamma}{\gamma+1} \cdot \frac{(\frac{dR}{dt})^2}{a_o^2} = \frac{2\gamma}{\gamma+1}\ \frac{4}{25}\, S(\gamma)^2\, \frac{1}{a_o^2}\, (\frac{E}{\rho_o})^{2/5}\ t^{-6/5}$$

$$\frac{T_s}{T_o} = \frac{2\gamma(\gamma-1)}{(\gamma+1)^2} \cdot \frac{\left(\frac{dR}{dt}\right)^2}{a_o^2} = \frac{2\gamma(\gamma-1)}{(\gamma+1)^2}\frac{4}{25} S(\gamma)^2 \frac{1}{a_o^2}\left(\frac{E}{\rho_o}\right)^{2/5} t^{-6/5}$$

where a_o is the speed of sound and γ is the ratio of specific heats. Figure 1 shows the radius and surface temperature of the fire ball as a function of time. The straight line portions are calculated with Taylor's theory. The period after 10^{-2} seconds will be discussed more fully in the next section.

The radial dependence of the pressure and density behind the shock front are shown in Fig. 2. Taylor's calculations probably describe the shock front region of the fireball fairly well up to about 10^{-2} seconds. The value of $S(\gamma)$ is taken from Taylor's work, which was done with the rather unrealistic value for γ of 1.4. The density of air behind the shock front decreases as a high power of r, approximately as $(r/R)^8$. Hence most of the mass of the fireball at this stage is close to the surface. Note also from Fig. 2 that the interior pressure falls to a constant value of 0.38 times the shock pressure.

It is not expected that Taylor's theory, since it neglects radiation, will give a good description of conditions inside the fireball. However, a crude estimate can be made of the diffusive motion of the internal radiation front. After the strong shock forms, we know that the shock front moves much faster than the internal radiation front. At this time the mean free path of the radiation is falling

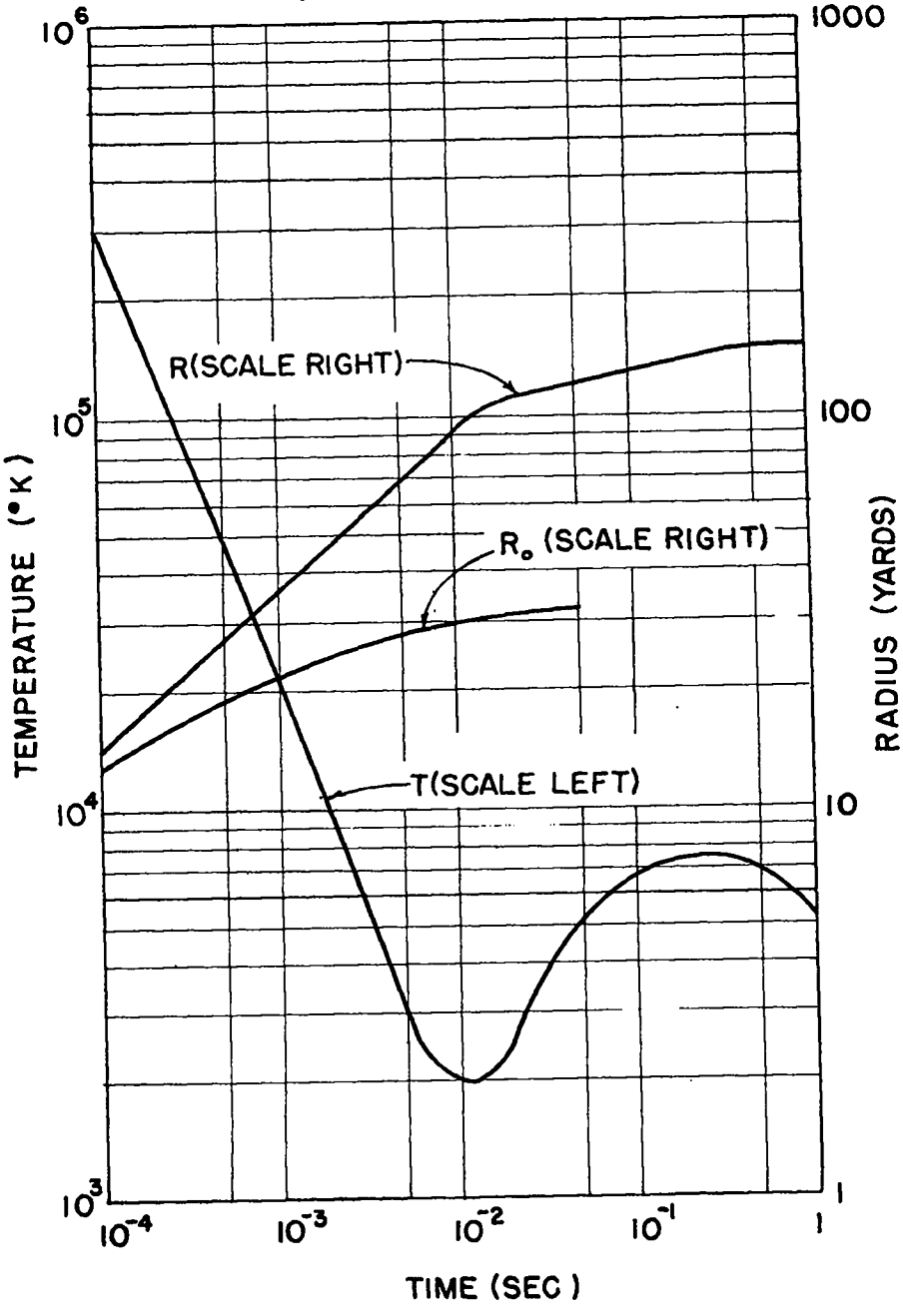

Fig. 1. Fireball radius R, radius of the internal radiation front R_o, and fireball surface temperature T as functions of time. These curves were calculated for a bomb with a yield of 10,000 tons of TNT.

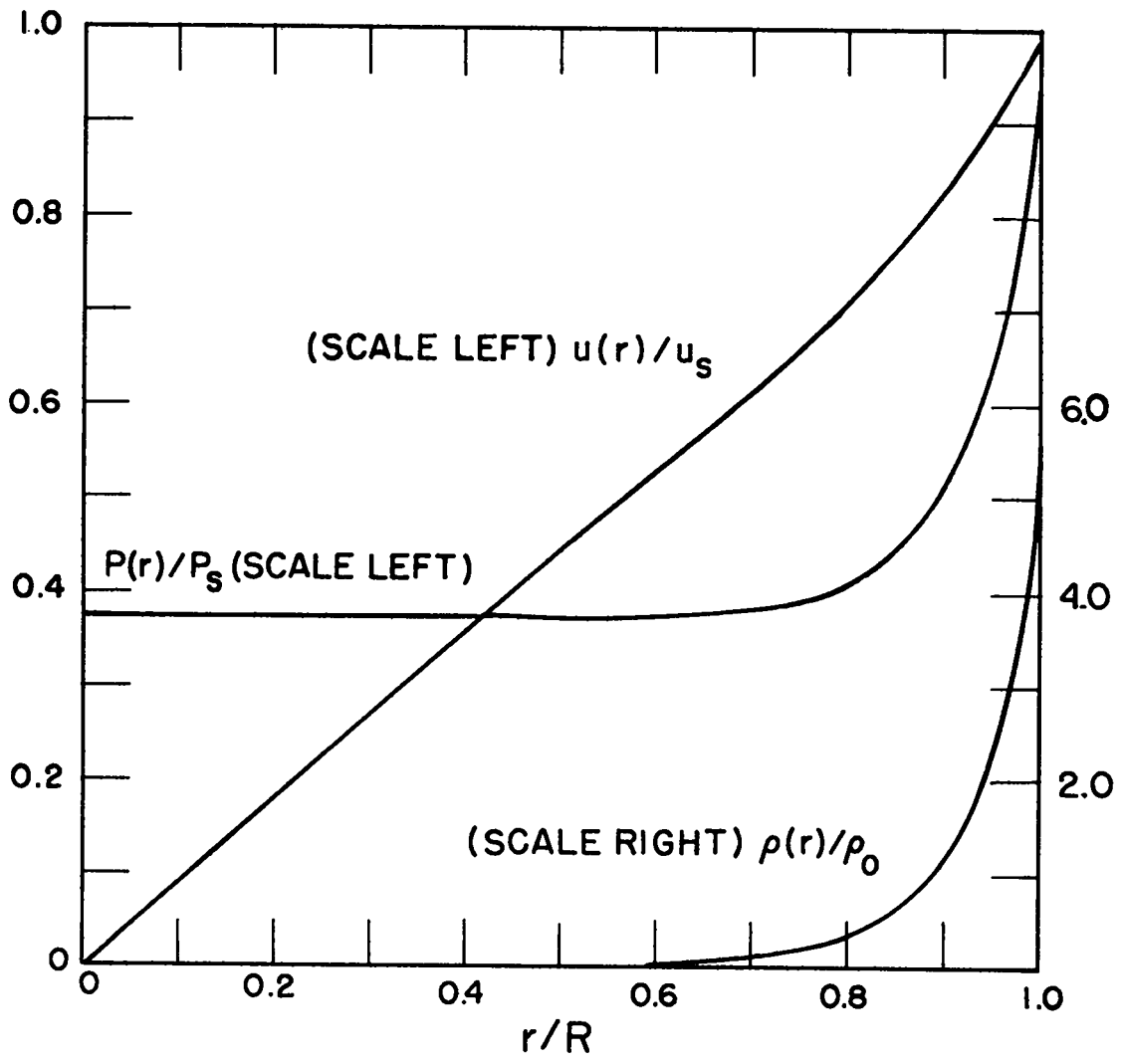

Fig. 2. Taylor's calculation of the pressure $P(r)/P_s$, the fluid velocity $u(r)/u_s$, and the density $\rho(r)/\rho_0$ behind the shock front as a function of r/R.

with the temperature. From Taylor's approximate solution for strong shocks, something is known about the variation of pressure and density behind the shock as a function of time. An approximate treatment of the internal radiation front can be made by calculating the transmission of radiation through a region which has these properties. The ambient temperature of this region is taken as zero (inconsistently), but this is permissible so long as the temperature of the isothermal core is much greater than the shock temperature. Figure 1 shows the results of this calculation, the radius of the internal radiation front R_o as a function of time.

2.4 The Minimum and Second Maximum

After 10 to 15 msec the temperature of the shock front is low enough that it ceases to be incandescent. At this time, which may be called the breakaway point, the shock front is no longer the surface of the fireball, but starts to move on ahead of the radiating gas of the interior. Since the shock no longer radiates, it becomes transparent to radiation from the much hotter gas inside. Thus the surface temperature of the fireball having reached a minimum, now starts to rise again and continues to rise until the temperature of the expanding isothermal core is reached. This gives a second maximum in surface temperature of 6,000 to 8,000°K at about 130 msec, which subsequently falls due to cooling of the gases by radiation and expansion.

The motion, as well as the existence, of the internal radiation front is understood qualitatively in terms of the dependence of the

opacity of air on temperature. The Rosseland mean free path, which controls the diffusive transport of radiation, increases with temperature above 50,000°K. As we have mentioned, the internal radiation front is formed at 300,000°K and thus as it diffuses out (through the air already affected by the shock) the radiation mean free path decreases at first as the temperature drops. Thus for a while there remains a well-defined radiation front moving more slowly as time increases. As the temperature of the core approaches 50,000°K, however, the diffusion mechanism breaks down since the mean free path now starts to increase as the temperature drops. The energy from the hot core is now radiated very strongly into the cooler air ahead.

The energy radiated by a core of 50,000°K or cooler is not lost to the blast. Most of it ($h\nu \gtrsim 6.6$ ev) is absorbed strongly in O_2 molecules and these exist in large numbers in air below 5000°K. Also in the shocked air there is a considerable amount of NO_2 between the temperatures of 2000 and 5000°K. In the explosion of a nominal bomb, on the order of 100 tons of NO_2 is formed. This compound absorbs most of the visible spectrum. Because of the absorption by excited O_2 and NO_2, the radiation flux actually strengthens the blast since it transports energy closer to the shock front, which of course tends to increase the pressure.

Although the core is radiating strongly before the time of the minimum, the air between core and shock front is so opaque that essentially none of this radiation gets through the shock front. After the

minimum the situation changes immediately. The transmission of air ahead of the core increases for three reasons:

(1) As the temperature of the core drops due to radiation and expansion, a larger fraction of its emitted radiation is below $h\nu = 6.6$ ev and is therefore transmitted by unexcited O_2. (Actually something less than 6.6 ev would be a better figure because less energy is required to dissociate vibrationally excited O_2 molecules and there are many of these at this temperature.)

(2) The NO_2 formed in the shocked air is limited to that material which was crossed by the shock at a shock temperature of 2000° or higher.

(3) The absorbing zone expands with time so that it becomes too tenuous to absorb a significant fraction of radiation.

Hence, soon after the shock front stops radiating at about the 100 meter radius, thermal radiation from the hot core is transmitted through the shock and the brightness of the fireball rises to a second maximum.

Spectrographic observations of the intensity of radiation from the fireball have been taken for most of the bombs tested. From these data the color temperature was obtained as a function of time. For this purpose, Wien's radiation law

$$U_\lambda = 8\pi\, hc\, \frac{1}{\lambda^5}\, e^{-\frac{hc}{\lambda kT}}$$

was assumed. Intensities of spectral radiation for several wavelengths were recorded on a spectrograph. The quantity $\ln U_\lambda \lambda^5$ was plotted against $1/\lambda$. The slope of this curve yields the temperature. The errors due to using the above approximation to the Planck radiation law are only a few percent at the most. Figure 3 gives the color temperature curve so obtained for the shot of March 17, 1953, a nuclear device of close to nominal size. This curve is typical of what is usually obtained. For larger bombs the minimum comes later and the second maximum comes later and lasts longer.

2.5 Importance of the Minimum

The minimum is the dividing line between two different kinds of spectra observed in nuclear explosions. Before the minimum one sees only radiation from the shock front surface of the fireball, and it is impossible to see into the interior. After the minimum one sees radiation from well behind the shock front, and in effect looks deeper into the fireball as time passes. In this late period the radiation passes through a much greater thickness of shocked and disturbed air, and hence the spectrum is expected to be much different. It should be noted that though the early period before the minimum is hotter, the late period is of far greater duration (up to 3 sec). In fact the energy released in the form of thermal radiation before the minimum is only about 0.3% of the total energy of the bomb, i.e., only about 1% of the total energy released as radiation.

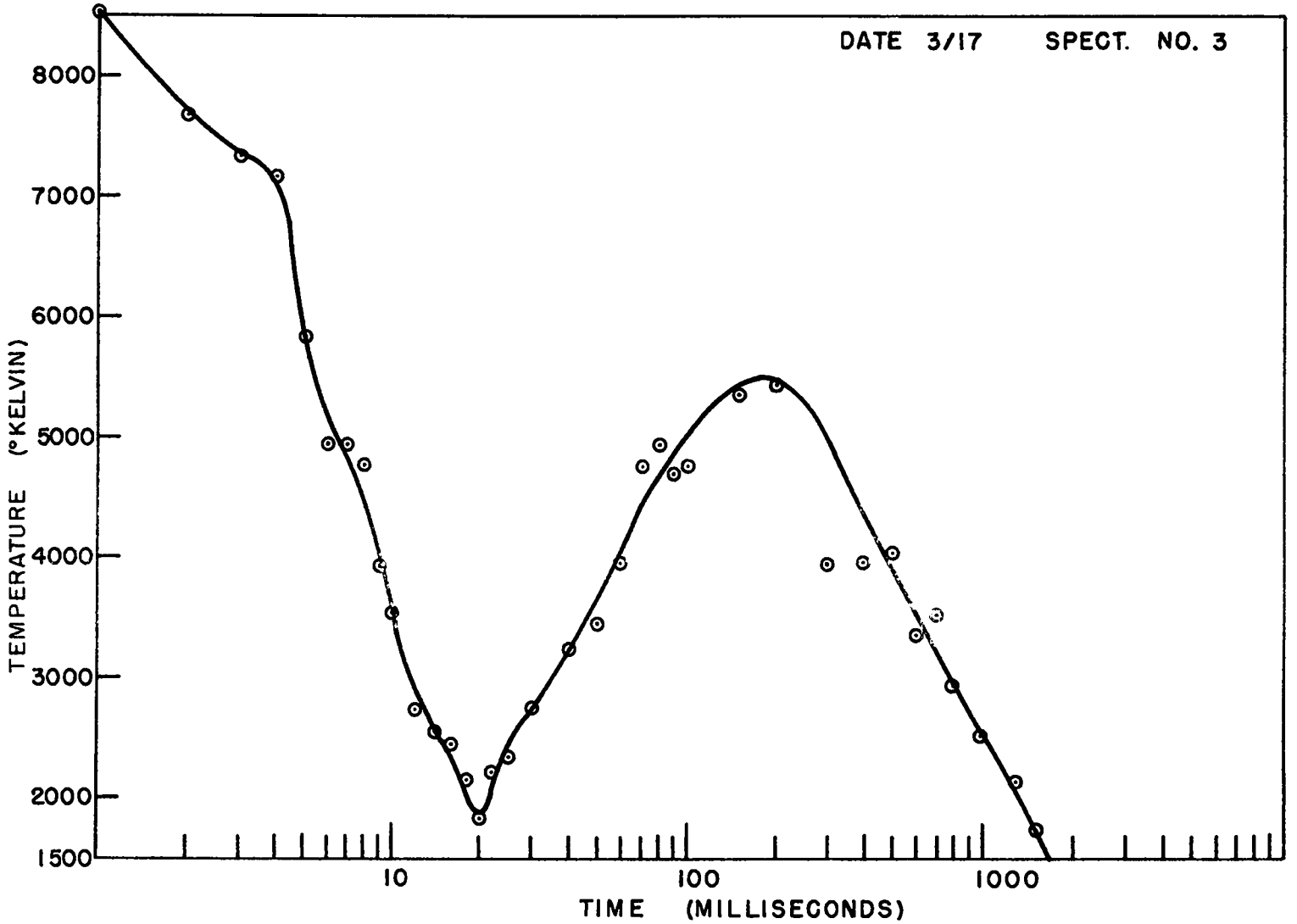

Fig. 3. Color temperature of the fireball surface as a function of time (from NRL-4356).

2.6 Scaling Laws

In discussing atomic bombs of different yields it is convenient to relate the characteristics of one bomb to those of a nominal bomb by simple scaling laws. The validity of these scaling laws depends on the hydrodynamical equations which apply to shock waves. From these it is possible to show that two explosions having the same initial conditions differ only with respect to a scaling factor applied to both distance and time. The success of scaling in the case of atomic bombs of different masses and constituents as well as yields is due primarily to the high concentration of energy which they produce. This means that although the two explosions are dissimilar in the very early stages in which the bomb masses are comparable with the air engulfed, these masses soon become negligible with respect to the mass of air engulfed by the shock wave. The two systems may then both be considered with reasonable precision to have originated from a point source or, more correctly, from small isothermal spheres which have been generated by the intense heating of the air by the bombs. On the basis of the foregoing argument, the state variables, i.e., pressure, temperature, and density, can be written as functions of distance and time for any atomic explosion, once they are given for a specific explosion, by scaling all distances and times by the cube root of the ratio of the energy yields. Thus:

$$\frac{r}{r_o} = \left(\frac{E}{E_o}\right)^{1/3}$$

and

$$\frac{t}{t_o} = \left(\frac{E}{E_o}\right)^{1/3}$$

where E_o, r_o, and t_o apply to the reference explosion, in this case a nominal atomic bomb.

It is of interest to examine some of the various radiation effects to see how they scale for blasts of different sizes.

According to the discussion of Section 2.1 the radiation expansion phase should end when the temperature drops to about 300,000°K For explosions in which the mass of the materials can be neglected, the volume of air contained at this stage varies directly as the yield and thus the radius varies as the cube root of the yield, or $R_o \sim E^{1/3}$, where R_o is the initial shock radius. The energy loss due to radiation in this early period is negligible.

The energy radiated through the shock front during the time that it radiates as a black body depends essentially on $4\pi R^2\, dR$, and hence varies directly as the explosion energy.

3. DESCRIPTION OF THE SPECTRA

3.1 The Teller Light

At the very beginning of the explosion there is an emission spectrum called the Teller light lasting a few microseconds. It consists chiefly of the second positive group of N_2 and N_2^+ bands. The

spectrum of the Teller light appears to be very similar to that of an ordinary glow discharge in air. The excitation is presumably through secondary electrons ejected by gamma rays, and hence should be proportional to the gamma radiation. The decay of the Teller light lasts some microseconds after the decay of gamma radiation because there is an afterglow which extends the emission over a finite time even with an instantaneous burst of gamma rays.

3.2 Early Absorption Spectrum

Before the Teller light fades out, the light from the fireball appears with a continuous spectrum. It rises to the first maximum at about 300 μsec and then decreases to the minimum at about 12 msec. The time of the minimum is later for larger and earlier for smaller bombs. During this early time the continuous background is modified by absorption lines and bands which can be attributed to air and reaction products formed in the air ahead of the shock front (mostly by gamma ray excitation). Usually no lines due to bomb constituents are observed before the minimum.

3.3 Late Absorption Spectrum

After the minimum the intensity rises to a broad maximum at about 130 msec, and then declines gradually. During this period the spectrum is dominated by absorption lines due to bomb constituents, chiefly iron. The air absorption is still present, and it depends on the particular bomb whether or not in certain parts of the spectrum the

metallic absorption predominates. Some emission lines may appear also. They seem to be localized in certain parts of the fireball only.

3.4 Formation of Unusual Compounds

The air between the fireball and the observer, particularly close to the fireball, is not normal air since it has been influenced by gamma rays, neutrons, and ultraviolet photons. These modify the air by ionizing and exciting O_2 and N_2 molecules. Secondary reactions are initiated which produce such substances as NO, NO_2, HNO_2, N_2O, O_3, and OH, which are not normally present in the atmosphere. In the later period the light from the fireball is seen through air disturbed to an even greater extent because it has been traversed by the shock wave, which gives rise to new conditions for the formation or destruction of these strange molecules.

Low dispersion streak spectrograms at intervals of 1.7 msec were taken for the shot of April 18, 1953, a bomb of slightly above nominal size. The spectral region covered is 3000 to 6000 A. Microphotometer traces were made of these spectrograms. Six of these traces are given in Figures 4 through 9 to illustrate the gross changes of the spectra with time. The first, labeled as taken at 0.1 msec, is about the time of the first maximum. The second is characteristic of the time between the first maximum and the minimum. The strong absorption by HNO_2 at these early times is particularly evident. The third at 15.4 msec shows the spectrum at the minimum. The fourth at 49.4 msec shows

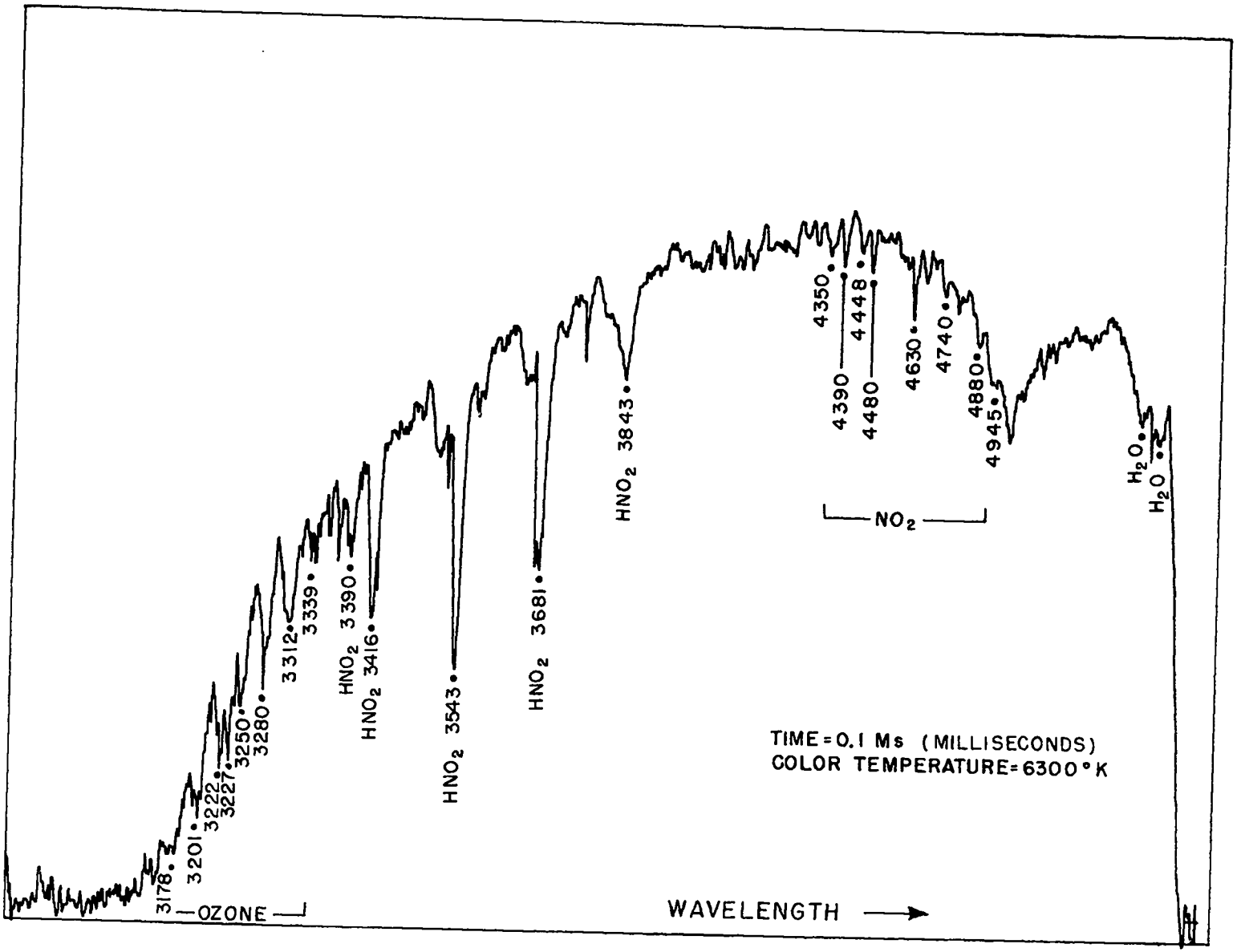

Fig. 4. Microphotometer of a low dispersion spectrogram at 0.1 msec for shot of April 18, 1953 (from NRL-4378).

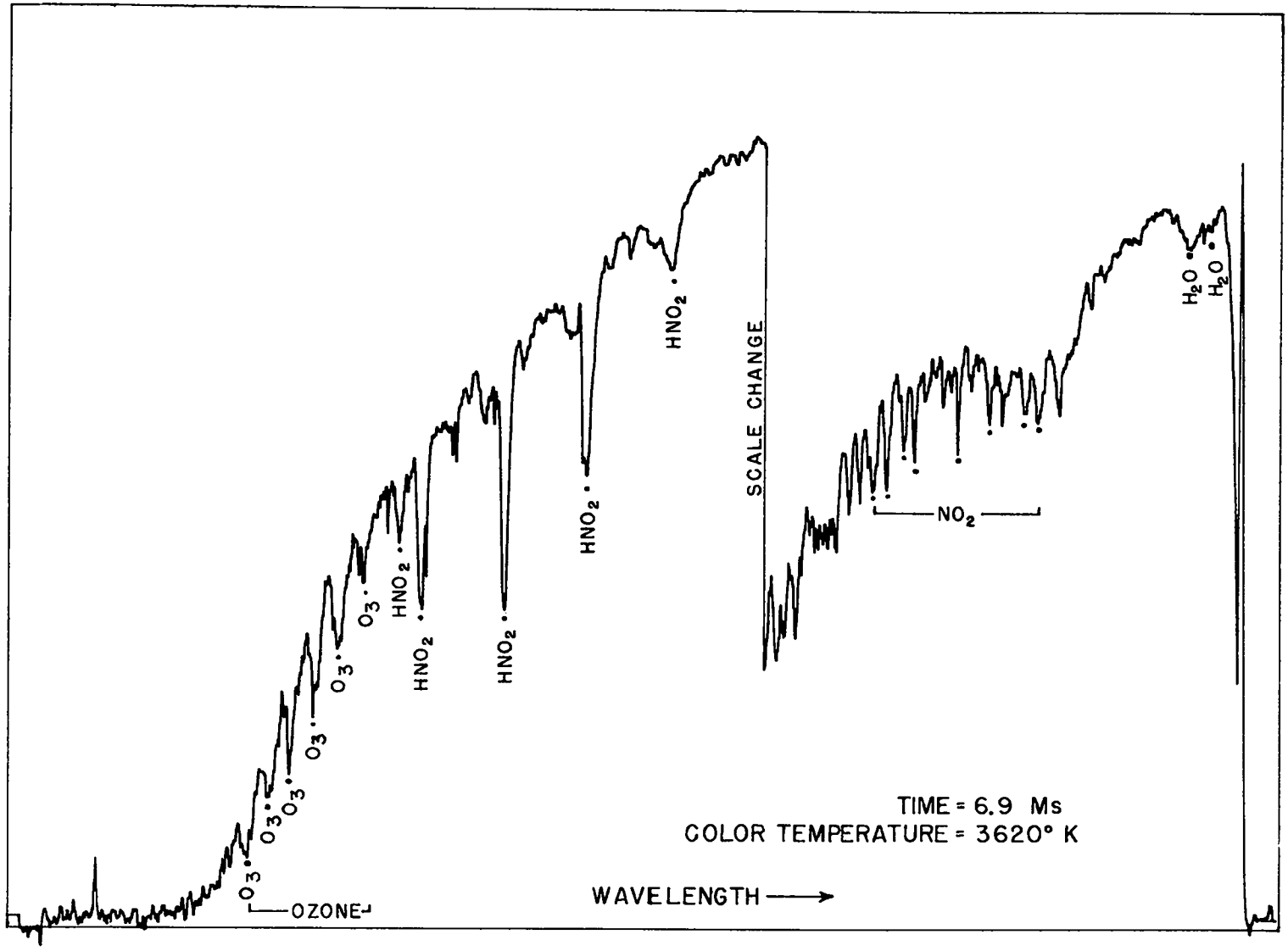

Fig. 5. Microphotometer trace of a low disperion spectrogram at 6.9 msec for shot of April 18, 1953 (from NRL-4378).

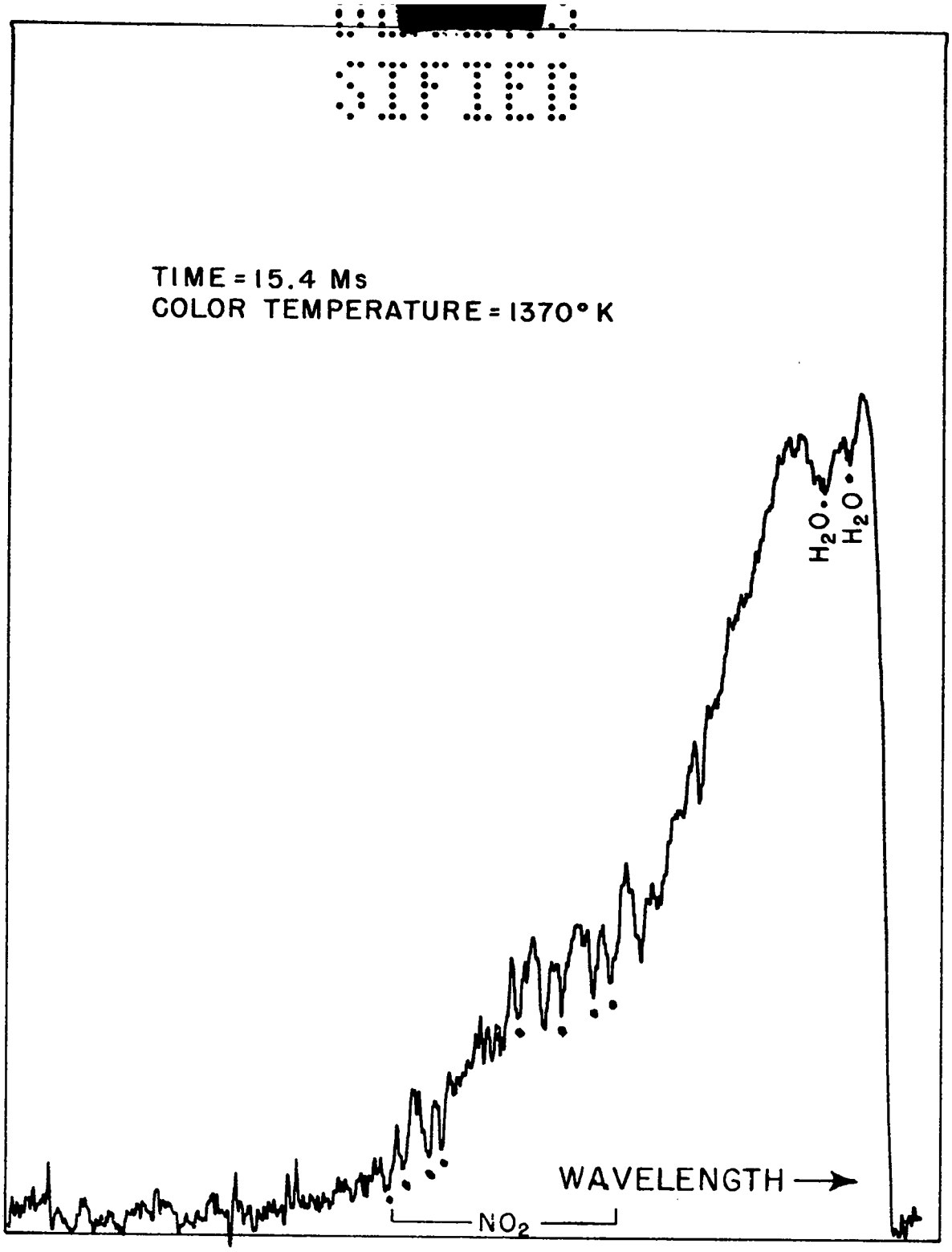

Fig. 6. Microphotometer trace of a low dispersion spectrogram at 15.4 msec for shot of April 18, 1953 (from NRL-4378).

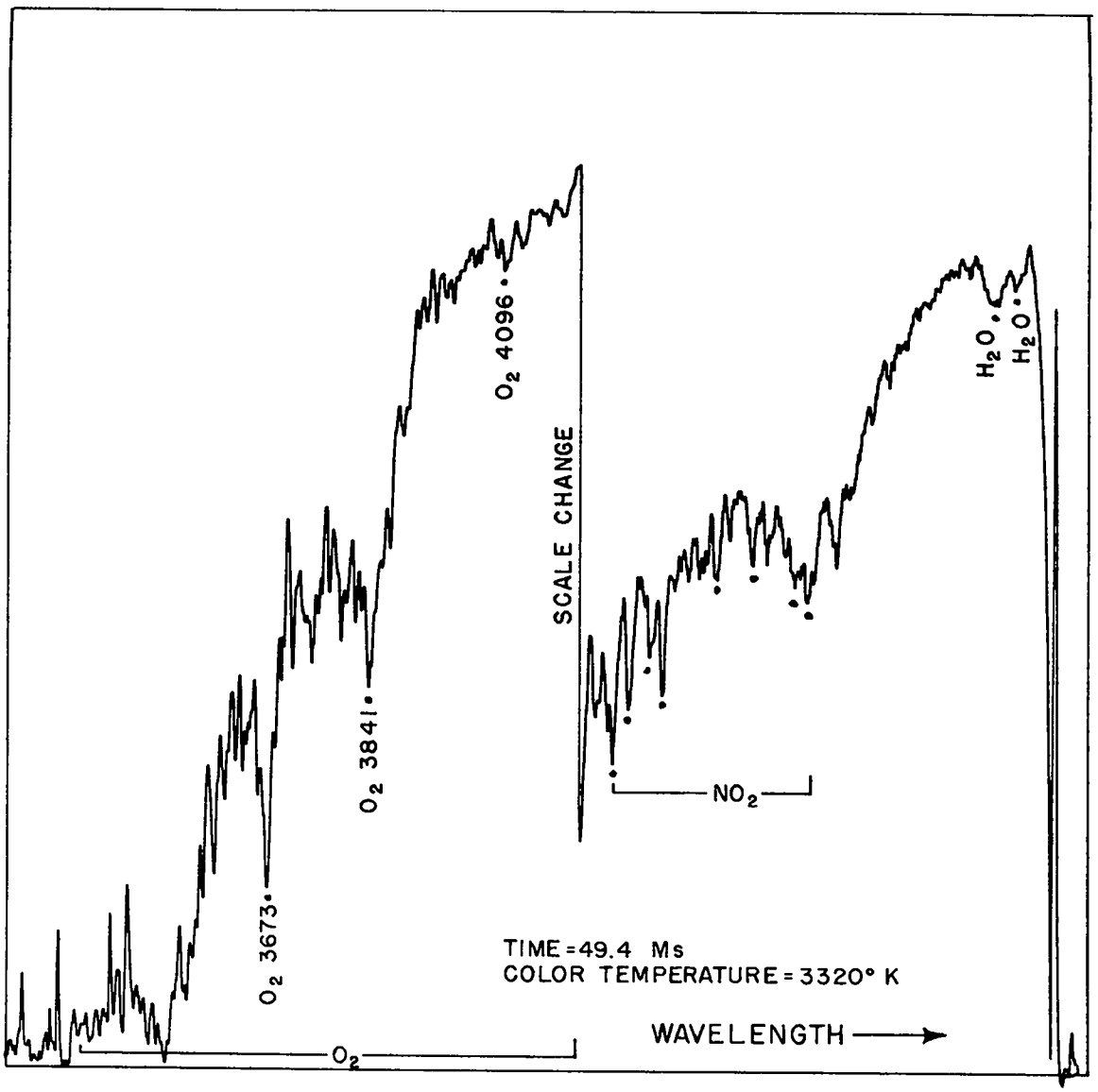

Fig. 7. Microphotometer trace of a low dispersion spectrogram at 49.4 msec for shot of April 18, 1953 (from NRL-4378).

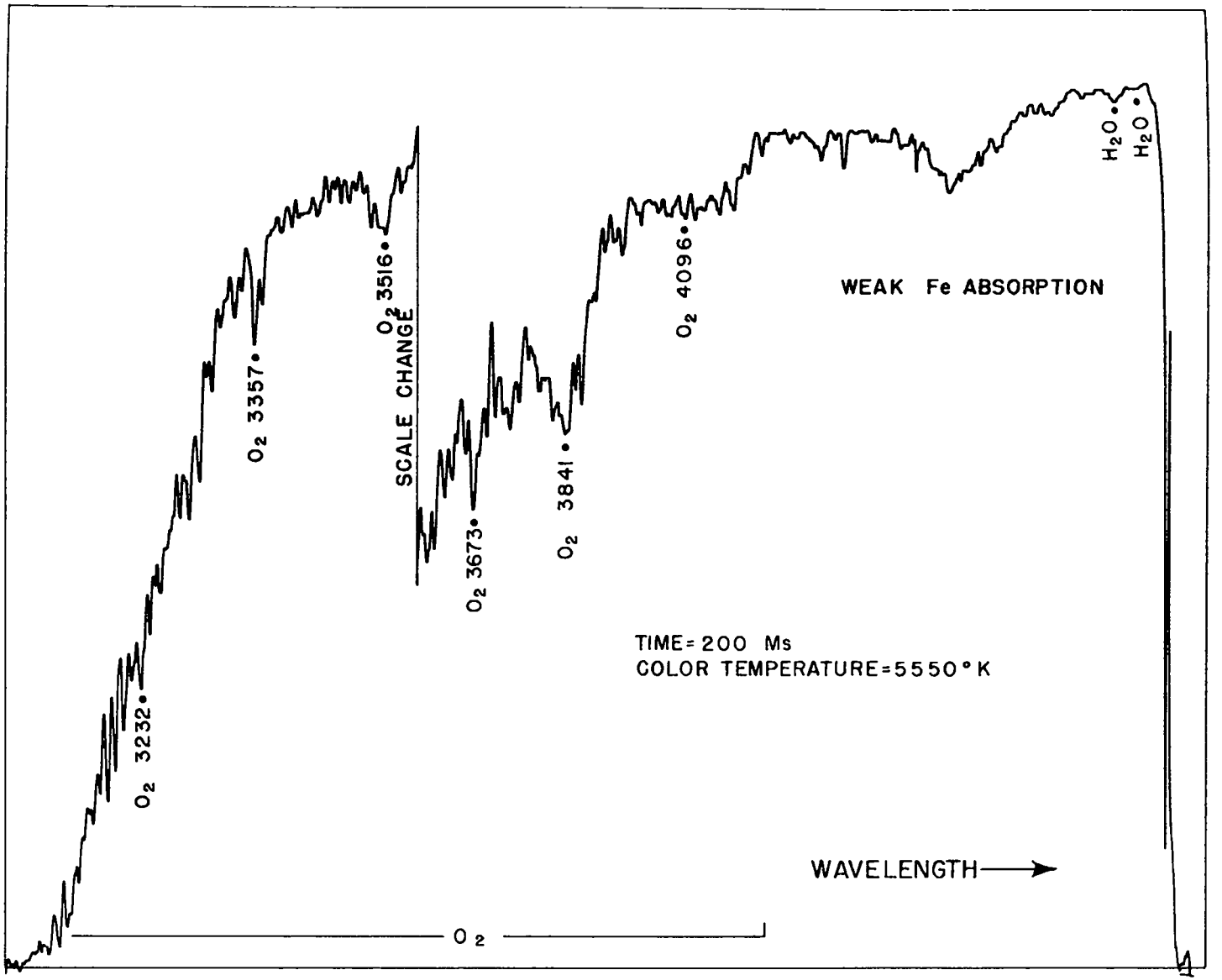

Fig. 8. Microphotometer trace of a low dispersion spectrogram at 200 msec for shot of April 18, 1953 (from NRL-4378).

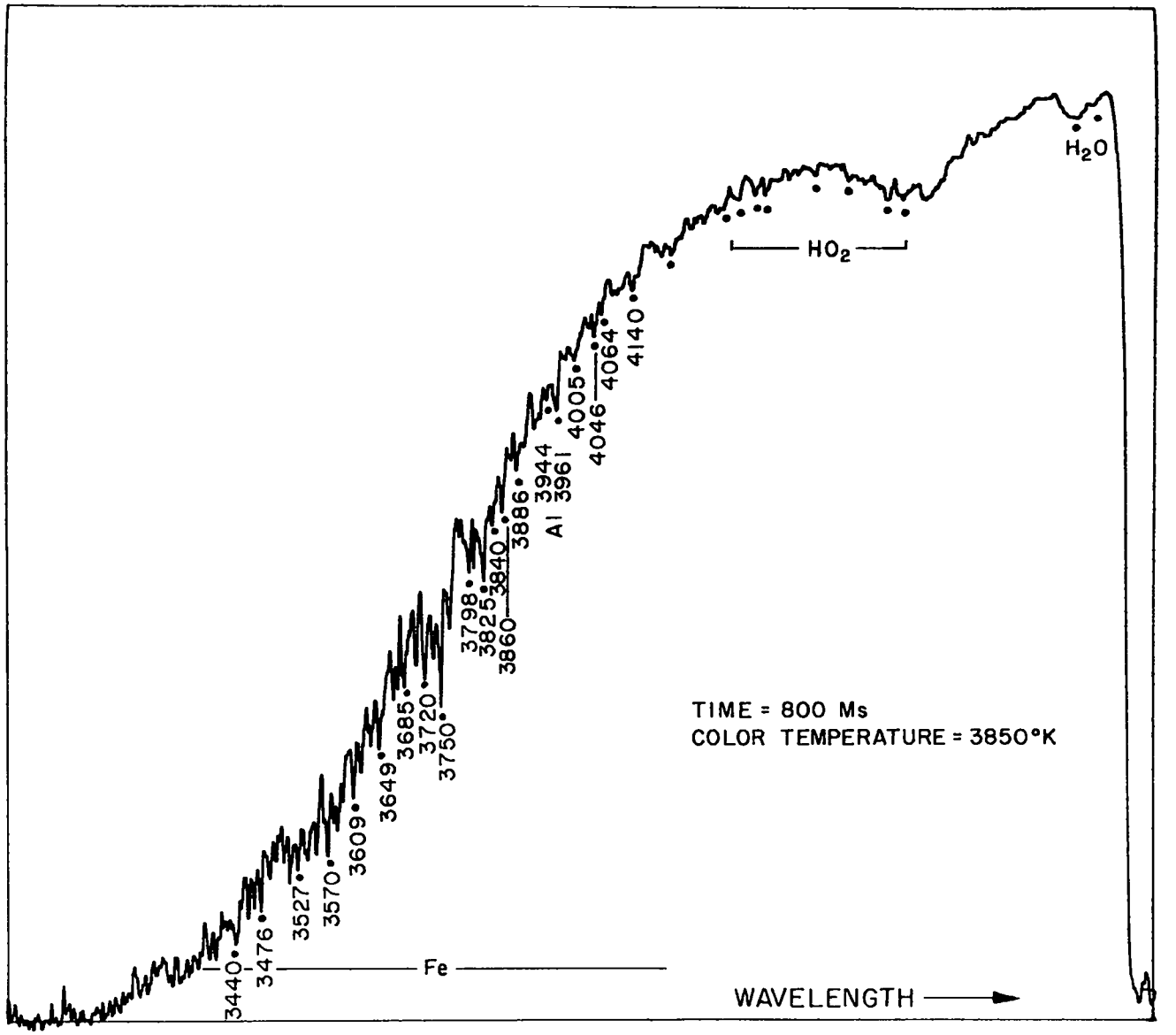

Fig. 9. Microphotometer trace of a low dispersion spectrogram at 800 msec for shot of April 18, 1953 (from NRL-4378).

the spectrum at a time between the minimum and the second maximum. Absorption by O_2 is most noticeable. The fifth at 200 msec is characteristic of the second maximum. Absorption by metals, particularly iron, is beginning to show up. In the sixth at 800 msec, well past the second maximum, absorption by metals is the most important feature. It should be pointed out that there is an uncertainty of 1.7 msec in the time of the initial exposure, because it was not possible to synchronize the first exposure with zero time.

3.5 O_2 Bands in Early and Late Spectra

A characteristic difference is seen in the O_2 absorption band spectra of the early and late periods. In the early period there are bands indicating absorption by oxygen molecules in high vibrational quantum states. The intensities are low so that these bands do not show up on the low dispersion spectra of Figs. 4 and 5. From the observed intensities one gets the remarkable result that the vibrational temperature is around 3000° while the rotational temperature is only around 400°. As was shown in Sec. 2, this non-equilibrium excitation must refer to the region between the luminous shock front and the observer. It may be due to photoexcitation or, more likely, excitation by electrons. Secondary electrons produced by gamma rays or neutrons collide with normal O_2 molecules, thus exciting them to high vibrational states. This process will be further discussed in Sec. 4.2.

In the late period the O_2 band spectrum is much more intense, and indicates equal vibrational and rotational temperatures. The

reason is that one is now seeing absorption by O_2 molecules between the shock front and the radiating core. Molecules engulfed by the shock front have an equilibrium excitation of their vibrational and rotational modes corresponding to the temperature behind the shock front.

3.6 Lines Due to Normal Air

The spectrum of normal air is not very interesting for this report and will be discussed only briefly. The observed lines are chiefly the atmospheric absorption bands at 7596, 6867, 6277, 5788, and 5380 A and the water vapor absorption bands which extend with increasing intensity from about 5700 A to the infrared. These bands do not contribute anything to the knowledge of the explosion but must be accounted for in order to facilitate identification of the "interesting" lines. The atmospheric O_2 and H_2O absorption bands were originally known as terrestrial lines in the solar spectrum. Our knowledge of them is not perfect, particularly of the H_2O bands, but a fairly recent detailed study of the O_2 bands is available.[4] The data from the solar spectrum are not adequate for two reasons. First, there are many interferences with solar lines. Second, there is considerably more air between many of the bomb explosions and the observer (5 to 15 miles) than between the sun and the observer (effectively 5 miles).

Nitrogen and rare gas constituents have no absorption in the accessible region of the spectrum. CO_2 absorbs in the infrared, but not strongly enough below 9000 A to show.

---

[4] L. Herzberg and H. D. Babcock, Astrophys. J. 108, 167 (1948).

4. SCHUMANN-RUNGE BANDS OF O_2

4.1 Excited O_2

Normal oxygen absorbs weakly in the extreme red (atmospheric absorptions bands), in the region between 2400 and 2600 A (Herzberg absorption bands), and strongly below 1860 A. Figure 10 shows the absorption coefficient of air, mainly due to oxygen, at 300°K and one atmosphere.[5] The absorption below 1860 A is due to transitions from the normal vibrationless state of the molecule ($X^3\Sigma$) to the upper state ($B^3\Sigma$) of the so-called Schumann-Runge bands. Figure 11 shows the potential energy curves of these two electronic states. In cold air the bands from the vibrational ground state, v = 0, are the only ones that can occur in absorption with any intensity.[6]

Looking at Figure 11 and applying the Franck-Condon principle, one sees that the most likely transitions from the ground vibrational state to the upper electronic state require an energy greater than the dissociation energy of the molecule in the upper state, even though there are several possible vibrational levels in the well of the upper curve. These vibrational states of the upper curve can be reached with ease only from higher vibrational states of the lower curve. Stueckelberg[7] has calculated the transition probability and corresponding absorption

---

[5] E. G. Schneider, J. Opt. Soc. Amer. 30, 128 (1940).
[6] H. P. Knauss and S. S. Ballard, Phys. Rev. 48, 796 (1945).
[7] E. C. G. Stueckelberg, Phys. Rev. 42, 518 (1932).

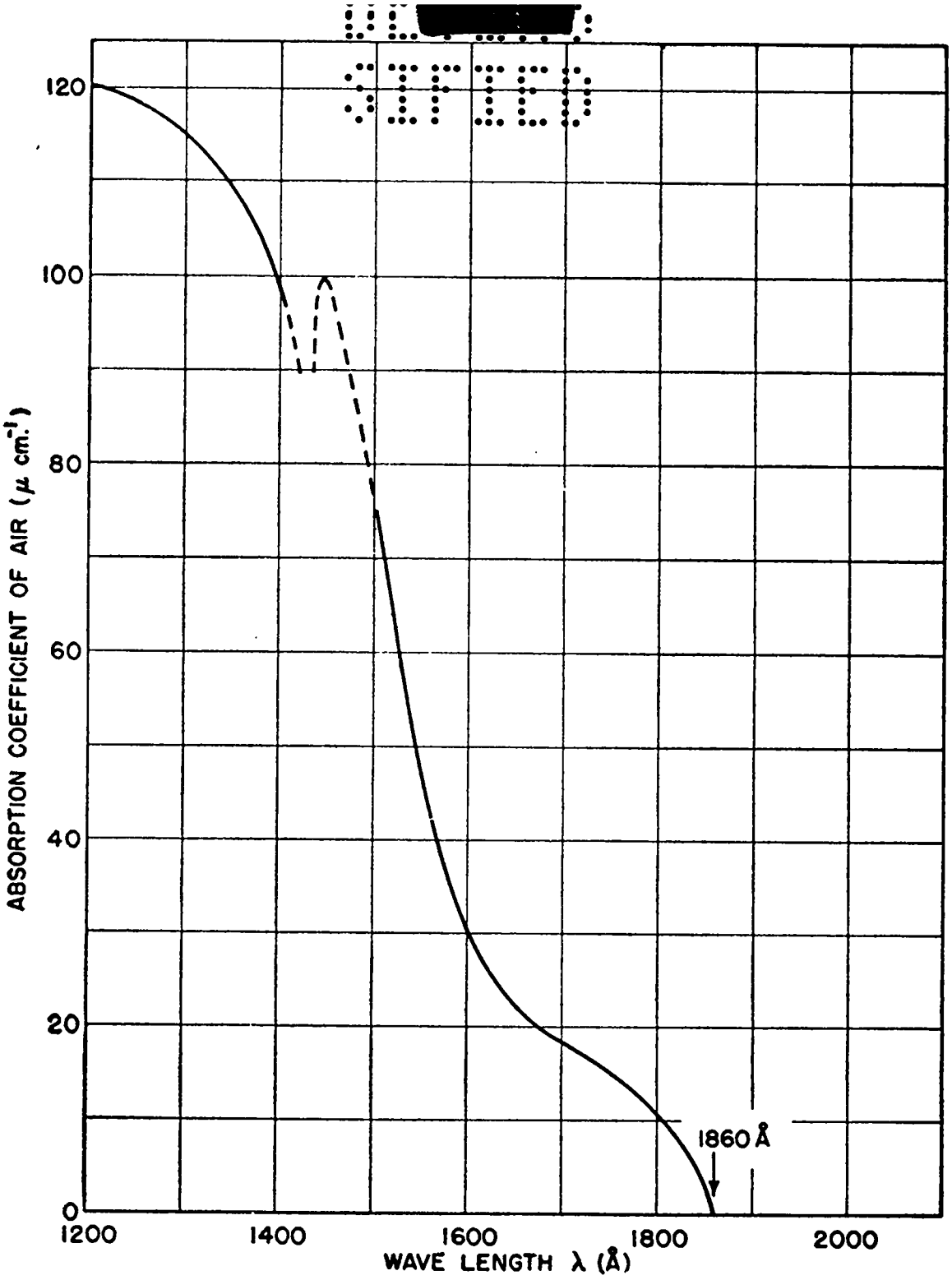

Fig. 10. Absorption coefficient of air vs wavelength at 300°K and 1 atmosphere (from The Effects of Atomic Weapons).

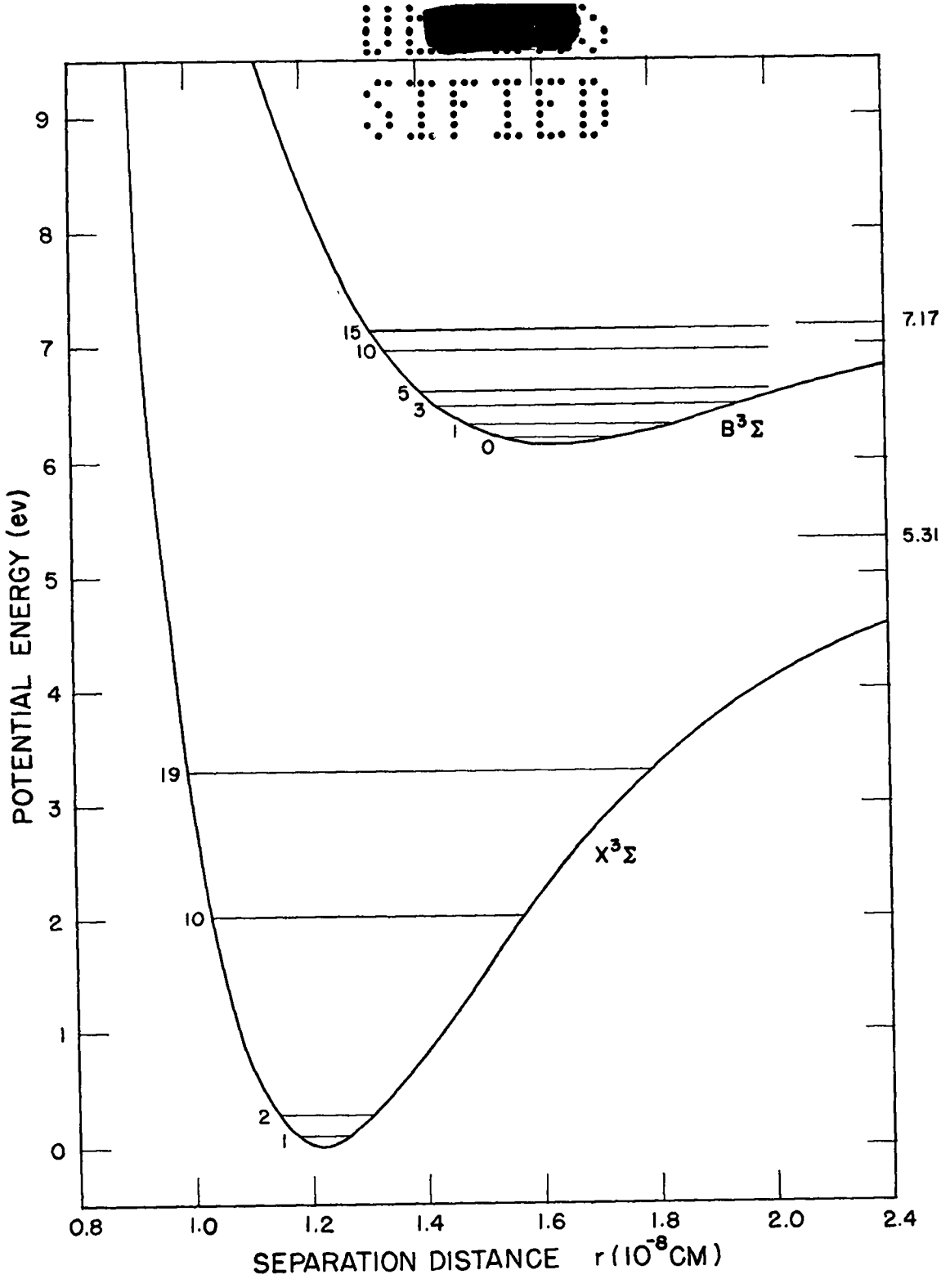

Fig. 11. Potential energy curves for O_2 in normal and excited electronic states.

coefficient for transitions from the ground vibrational states to the dissociated upper state. For air at higher temperatures enough of the O_2 molecules are excited to the higher vibrational states so that longer wavelengths than 1860 A are also strongly absorbed. It is this absorption that takes out most of the radiation from the core of the fireball.

Quantitative measurements of the strength of the absorption bands in air at room temperature were made by Lameris.[8] More bands of this system are observed in emission[9] and in absorption in heated O_2, so that the position of a large number of bands and their rotational structure is fairly well known. Füchtbauer and Holm[10] heated the oxygen to 1050°K and found that the absorption bands extended to 2200 A and that those with the longest wavelength were due to absorption by molecules with five quanta of vibrational energy. The Schumann-Runge bands are not found in the ordinary spectrum of the sun but some of the bands have been detected in the sun spot spectra.[11]

In the early stages of an atomic explosion the oxygen absorption bands are a very conspicuous feature in the ultraviolet part of the high dispersion spectra. They do not show in the low dispersion spectra of Figures 4 and 5 because the resolution of these low dispersion

---

[8] A.J. Lameris, Intensiteitsmetingen in Het Ultraviolette Absorptiespectrum van Zuurstof. Dissertation, Groningen, 1938.

[9] W.Lochte-Holtgreven and G.H. Dieke, Ann. phys. 3, 937 (1929); M.W. Feast, Proc. Phys. Soc. London A62, 114 (1949); A63, 549 (1950).

[10] C. Füchtbauer and E. Holm, Physik. Z. 26, 345 (1925).

[11] H. D. Babcock, Astrophys. J. 102, 154 (1945).

spectrographs is not high enough to reveal such sharp lines. In the later stages these bands are present with much greater intensity, and do show up on the low dispersion spectrographs (Figures 8 and 9), but the identification is harder because they fall between strong iron absorption lines. Table 1 gives the wavelengths of bands known from laboratory experiments and those observed in the spectra of nuclear explosions.

4.2 Schumann-Runge Bands Before the Minimum

The bands that appear in the high dispersion spectra of this early period are chiefly the 0-13, 0-14, 0-15, 0-16, and 0-17 bands.* A few others show up more weakly, indicating absorption by molecules with up to 20 quanta of vibrational energy. Such high vibrational energies indicate either a very high temperature or a nonequilibrium excitation. An examination of the rotational band intensity distribution shows that the second alternative is correct.

The relative intensity distribution of the Schumann-Runge bands both in emission and absorption under various conditions has been calculated by Pillow.[12] The calculations are based on simplifying assumptions and the results cannot be relied on to be very accurate. They show, however, the general trend. Table 2 gives results of these calculations for absorption (a) at room temperature; (b) at 1350°, the

[12] M. E. Pillow, Proc. Phys. Soc. London A63, 940 (1950).

*The first number is the vibrational quantum number in the upper electronic state, the second that in the lower electronic state (initial state).

Table 1

THE SCHUMANN-RUNGE BANDS OF OXYGEN

Wavelengths of Origins or Heads

v' \ v''	0	1	2	3	4	5	6	7	8	9	10	11	12	13	14	15	16	17	18	19	20	21
0	2026 (0.10)	2092									2870	2983	3104	3233**	3370**	3517**	3673**	3841**	4021	4215		
1	1998 (1.00)	2062							2614	2711	2814	2923	3039	3164		3434	3583**	3742*	3913*	4096*	4292	
2	1971 (4.85)	2034						2480	2569	2663			2971	3093	3223	3357*	3500**			3987	4173*	4373
3	1947 (15.2)	2007																				
4	1924 (43.2	1984																				
5	1902 (157)	1960 (1.12)	2021	2084	2151	2221																
6	1882 (300)	1938 (2.78)		2060	2125	2193																
7	1863 (565)	1918 (4.84)		2038	2101	2168																
8	1846	1900 (8.35)		2017	2080																	
9	1830	1884 (19.2)																				
10	1816																					
11	1803																					
12	1792																					
13	1782																					
14	1774																					
15	1768																					

The laboratory observations for v''<6 were made in absorption; those for v''>6 in emission.

Data underlined - Emission: Lochte-Holtgreven and Dieke.[9]
Absorption: Knauss and Ballard.[6]

Others - Emission: Feast.[9]
Absorption: Füchtbauer and Holm,[10] Lameris.[8]

**Found in absorption in early stages of shot of June 1, 1952.

*Same but weaker and identification needs checking.

The numbers in parentheses under the wavelengths are quantitative intensity measurements by Lameris[8] at a temperature of 17.5°C.

Table 2

CALCULATED INTENSITIES OF THE SCHUMANN-RUNGE SYSTEM OF O_2 AT VARIOUS TEMPERATURES

T = 300°K

v' \ v''	0
0	
1	
2	
3	
4	
5	1[K]
6	5[K]
7	20[K]
8	29[K]
9	51[K]
10	50[K]
11	78[K]
12	100[K]
13	90[K]
14	95[K]

K = bands observed in absorption in cold gas by Knauss and Ballard.

T = 1350°K

v' \ v''	0	1	2	3	4	5	6
0							
1							
2				1	1		
3			1	1	2	1	
4		1	3	4	3	1	
5	1	3[H]	6	6[H]	2[H]	1[H]	
6	2	8[H]	14	12[H]	8[H]	3[H]	1
7	8	16[H]	24	19[H]	8[H]	3[H]	1
8	12	27[H]	35	23[H]	11[H]	3[H]	
9	21	34	43	24	10	2	
10	20	43	45	24	8	1	
11	31	70	62	31	8	1	
12	40	88	67	30	7		
13	36	100	59	23	5		
14	38	77	55	19	3		

H = bands observed in absorption in heated gas by Füchtbauer and Holm.

T = 2300°K

v' \ v''	0	1	2	3	4	5	6	7	8	9
0						1	1	1	1	1
1					1	2	2	2	2	1
2				2	5	3	4	3	2	1
3			1	4	9	8	6	4	2	1
4		1	4	11	16	15	10	5	2	
5		3	9	19	11	15	14	6	1	
6	1	6	20	36	46	32	16	5	1	
7	3	12	36	56	47	38	16	3		
8	4	19	52	70	65	35	11	2		
9	8	25	64	72	61	27	6			
10	8	33	67	73	51	17	1			
11	12	49	92	91	49	13				
12	15	63	100	89	40	8				
13	13	72	87	70	28	3				
14	14	56	81	57	20	2				

Infinite Temperature

v' \ v''	0	1	2	3	4	5	6	7	8	9	10	11	12	13	14	15	16
0							1	3	7	19	40	62	87	94	72	48	21
1						1	2	4	9	14	17	11	1	4	23	72	100
2						1	3	6	10	12	7	2		2	6		11
3					1	2	5	7	11	8	3		3	6	5	2	1
4					2	4	8	12	10	4							
5					1	4	10	12	7	1	1						
6				1	5	9	13	10	3		4						
7			1	2	5	11	12	6		2	6						
8			1	2	7	10	9	4	1	6	8						
9			1	3	6	8	4		2	6	3						
10			1	3	5	5			3	2							

highest temperature reached by Füchtbauer and Holm; (c) at 2300°, the highest temperature at which laboratory experiments conceivably might be done; and (d) at infinite temperature where all vibrational levels are equally probable. Table 2, for infinite temperature, suggests that the strongest absorption is for the 0-12, 0-13, and 0-14 bands. The most intense bands observed are the 0-14 and 0-15, hence a quite high (several thousand degrees) vibrational temperature is suggested. Also from Table 2 it is expected that transitions to the upper vibrational ground state (v' = 0) are strongest, and that the transitions become unobservably weak for the higher upper vibrational states (v' > 2). The observed bands agree with this expectation.

There is evidence that Pillow's calculations cannot be relied on for quantitative details. The 0-16, 1-16, and 2-16 bands are given by Pillow in the ratio 21:100:11, and this ratio should be independent of temperature. Actually the 0-16 band is far stronger than the other two. Similarly 0-15 is much stronger than 1-15 although the calculated ratio is 48:72. Quantitative laboratory intensity measurements would be useful.

When we consider the rotational intensity distribution, it is seen that each band has only a relatively few lines--a fact which suggests low temperatures. With the present plates all that is justified is a rough estimate. For this purpose the 0-14 band, shown in Figure 12, is most favorable even though the R(K) and P(K-4) lines fall so nearly on top of each other that they cannot be separated. Figure 12

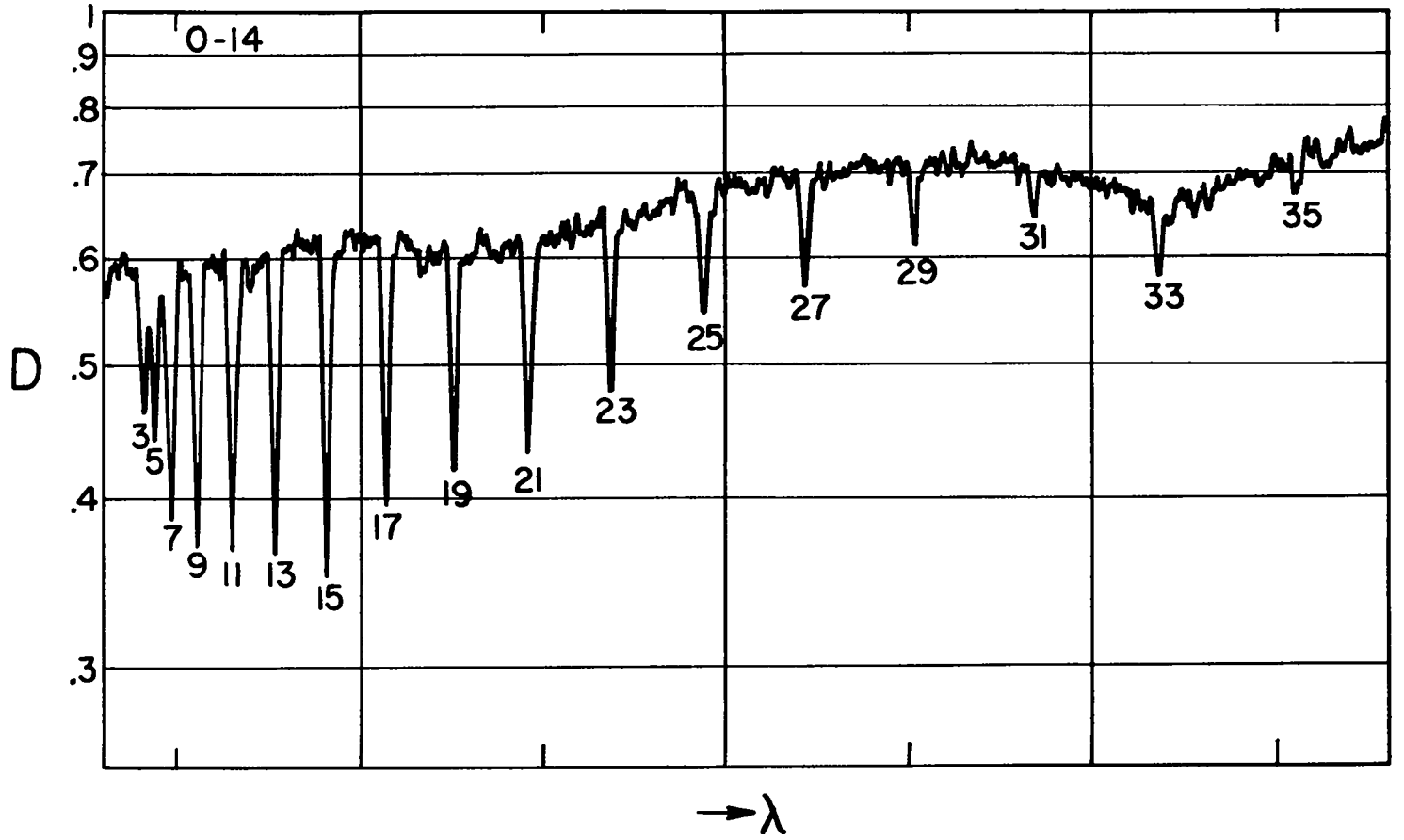

Fig. 12. Absorption by hot oxygen as recorded on the 2-meter Baird spectrograph in the first 20 msec of the shot of October 30, 1951. The rotational numbering is that of the R-branch. (From LA-1329)

is part of a photometer tracing of a high dispersion spectrograph taken during the first 20 msec of the shot of October 30, 1951. Figure 13 gives the calculated intensity distribution of rotational lines of this band at 400° and 3000°K. At 400°K, the maximum is near K = 13, and R(5) + P(1) and R(23) + P(19) have about the same intensity. This is true for the observed 0-14 band. Hence the rotational temperature is close to 400° or possibly a little lower.

The other strong O_2 bands are less suitable for determining the rotational temperature. For the 0-13 band the continuous background is rather weak. The 0-15 and 2-16 bands, shown in Figure 14, have a strong superimposed HNO_2 absorption. The rest of the bands are too weak. However, the conclusions reached from the 0-14 band are qualitatively confirmed by all the other bands.

To understand this difference between the vibrational and rotational temperatures it must be realized that one is seeing absorption by excited O_2 molecules in front of the shock front. The shock front itself gives continuous black body radiation ranging from T = 10,000° at the beginning down to 3000° at 10 msec for a nominal bomb. The excitation may be due to photons or to secondary electrons from gamma rays or neutrons. The secondary electrons excite the O_2 molecules, but during the collisions no substantial transfer of rotational angular momentum takes place* so that the rotational temperature

*Because of its small mass, an electron of several ev, hitting one of the O atoms in an O_2 molecule, has an angular momentum of only about one unit relative to the center of mass of O_2. Only this amount of angular momentum (at the most) can be transferred to the rotation of O_2.

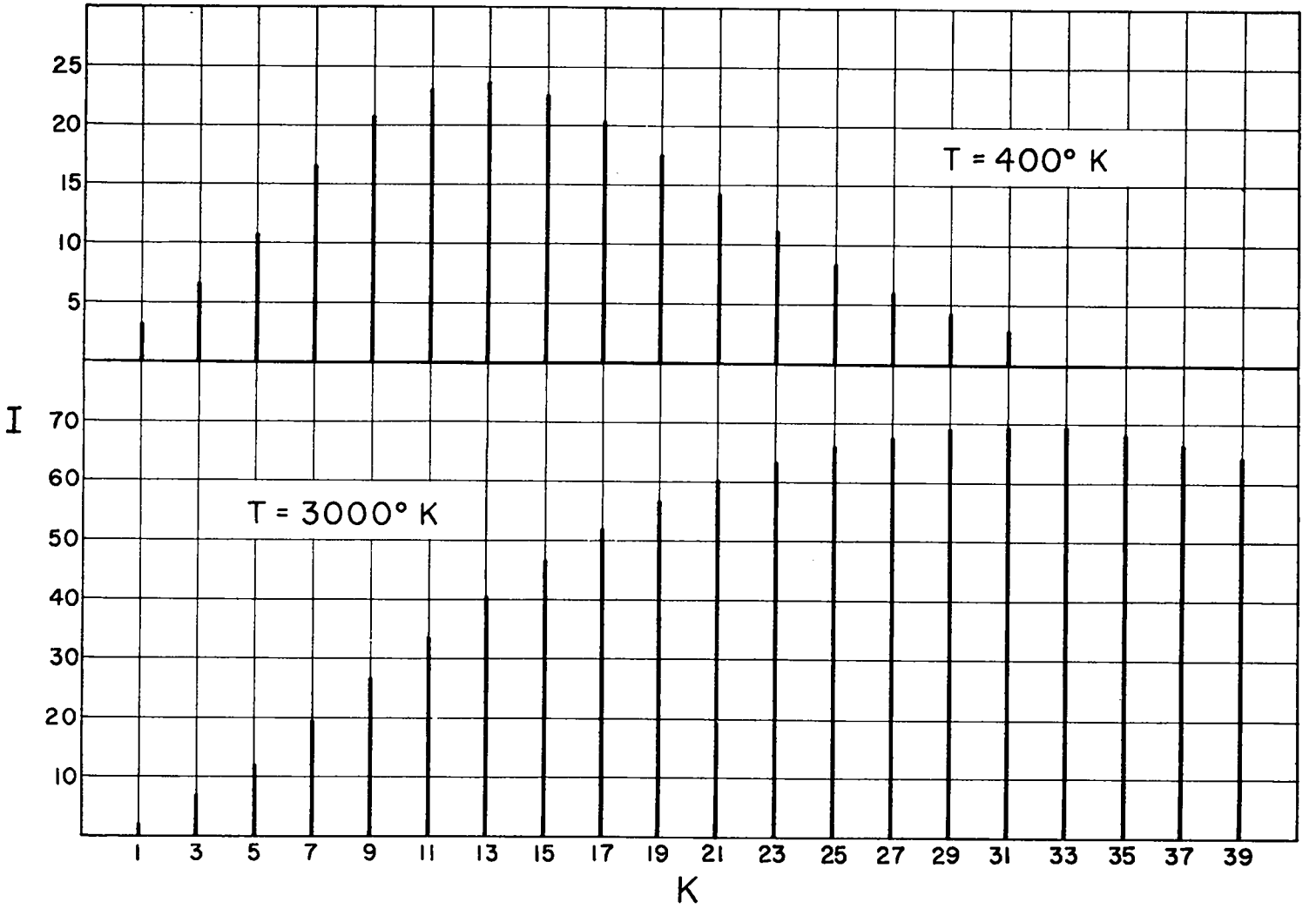

Fig. 13. Calculated distribution of intensities for the 0-14 band of O_2 at 400 and 3000°K (from LA-1329).

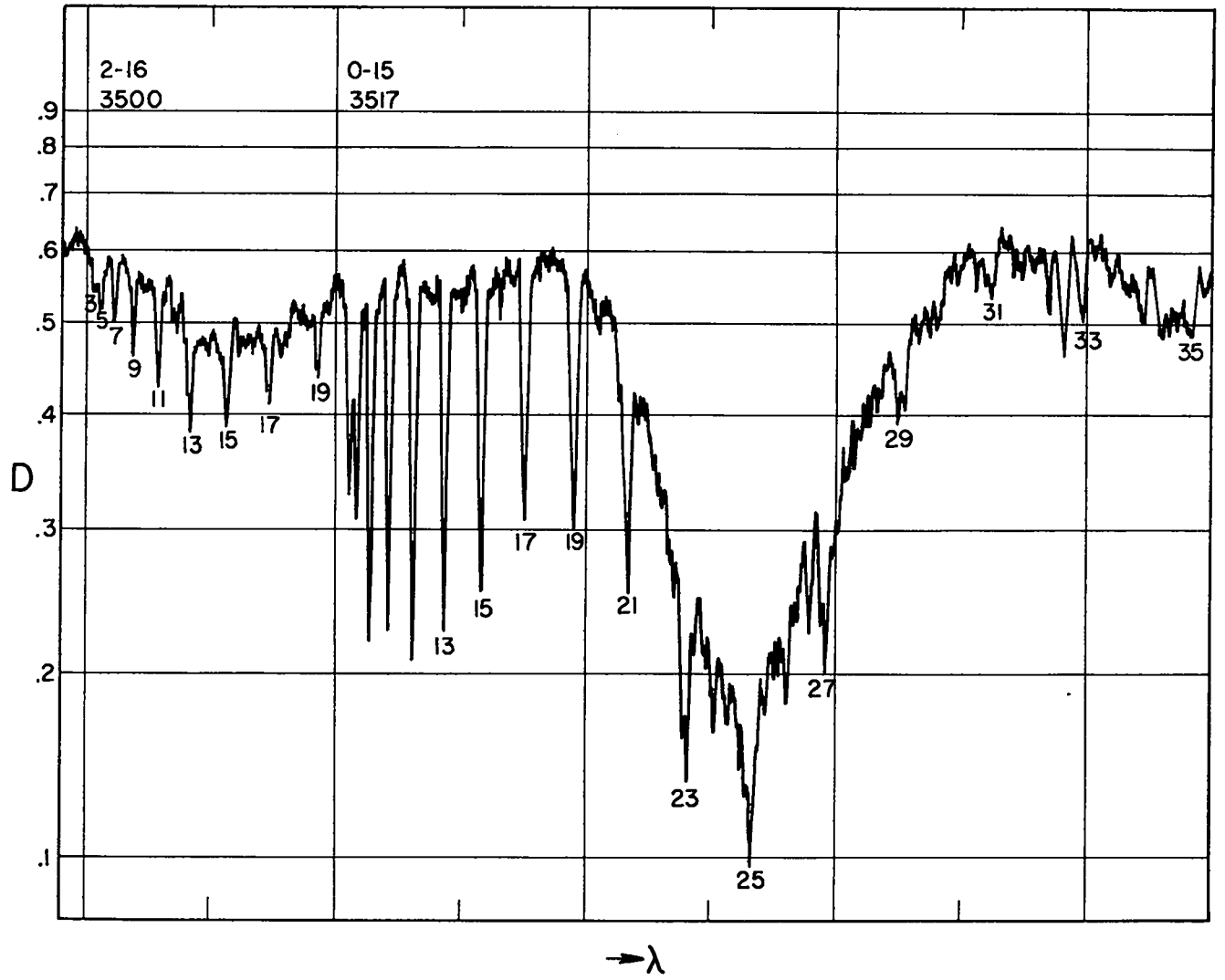

Fig. 14. The 0-15 and 2-16 bands of O_2 seen with light from the early period of the shot of June 1, 1952. The strong 3539 A HNO_2 band is superimposed on the 0-15 band and the weaker 3510A band on the 2-16 band. (From LA-1329)

remains essentially unchanged.

Electrons by preference will raise the O_2 molecules to the excited $B^3\Sigma$ state. Because of the Franck-Condon principle, a considerable amount of vibrational energy will be transferred simultaneously. According to Table 2, when $T = 300^\circ$ the most probable amount of vibrational energy in the excited state is 12 quanta. Many molecules will receive more than this amount, and a considerable portion will be dissociated. The molecules in the non-dissociated $B^3\Sigma$ state will return to the normal electronic state in a time interval of the order of 10^{-8} seconds with emission of radiation. Again using the Franck-Condon principle, many will land on a high vibrational state. Excitation by ultraviolet light (below 1860 A) would have essentially the same effect. However, the mean free path of photons of this wavelength is very small and for this reason it seems more probable that the primary agent is more penetrating radiation, gamma rays or neutrons, which produce secondary electrons which then cause the excitation. The O_2 molecules in the normal electronic state with a large excess of vibrational energy can lose this energy only by collisions. In the early stages of the explosion (5 msec or so) these excited molecules in front of the shock front have not had a chance to make many collisions. Hence in the early times there will be a fair number of vibrationally excited O_2 molecules available for absorption in air that is not yet genuinely hot.

4.3 Schumann-Runge Bands After the Minimum

In the later stages of the explosion (after 15 or 20 msec) the oxygen absorption bands are due to O_2 molecules between the shock front and the isothermal sphere. Excitation by the shock front causes a genuine temperature increase which produces an equilibrium between rotation and vibration. O_2 molecules originally excited to high vibrational states will have had a chance to make many collisions and thus convert excess vibrational energy into rotational and translational energy. Hence an equilibrium situation should be observed.

On the later spectra the same O_2 bands can be found as on the early spectra. They are not as conspicuous as on the early high dispersion spectra because of the large number of iron lines which occur in the same region and from anong which the O_2 lines have to be picked out. There will be many coincidences between O_2 and iron and other lines so that intensities are not very reliable. Nevertheless, a striking difference from the early spectra is apparent.

While during the first period the rotational lines of a band cannot usually be traced much beyond K = 30 notwithstanding a completely clear background, in the later spectra they can easily be traced to K = 80 and the maximum is definitely shifted to higher K values. Figure 15 shows a high dispersion tracing of the 0-14 band taken at the time of the second maximum for the shot of October 28, 1951. Comparing this figure with Figure 12 for the same band during the early period, one can see the difference. The maximum of the calculated intensity distribution

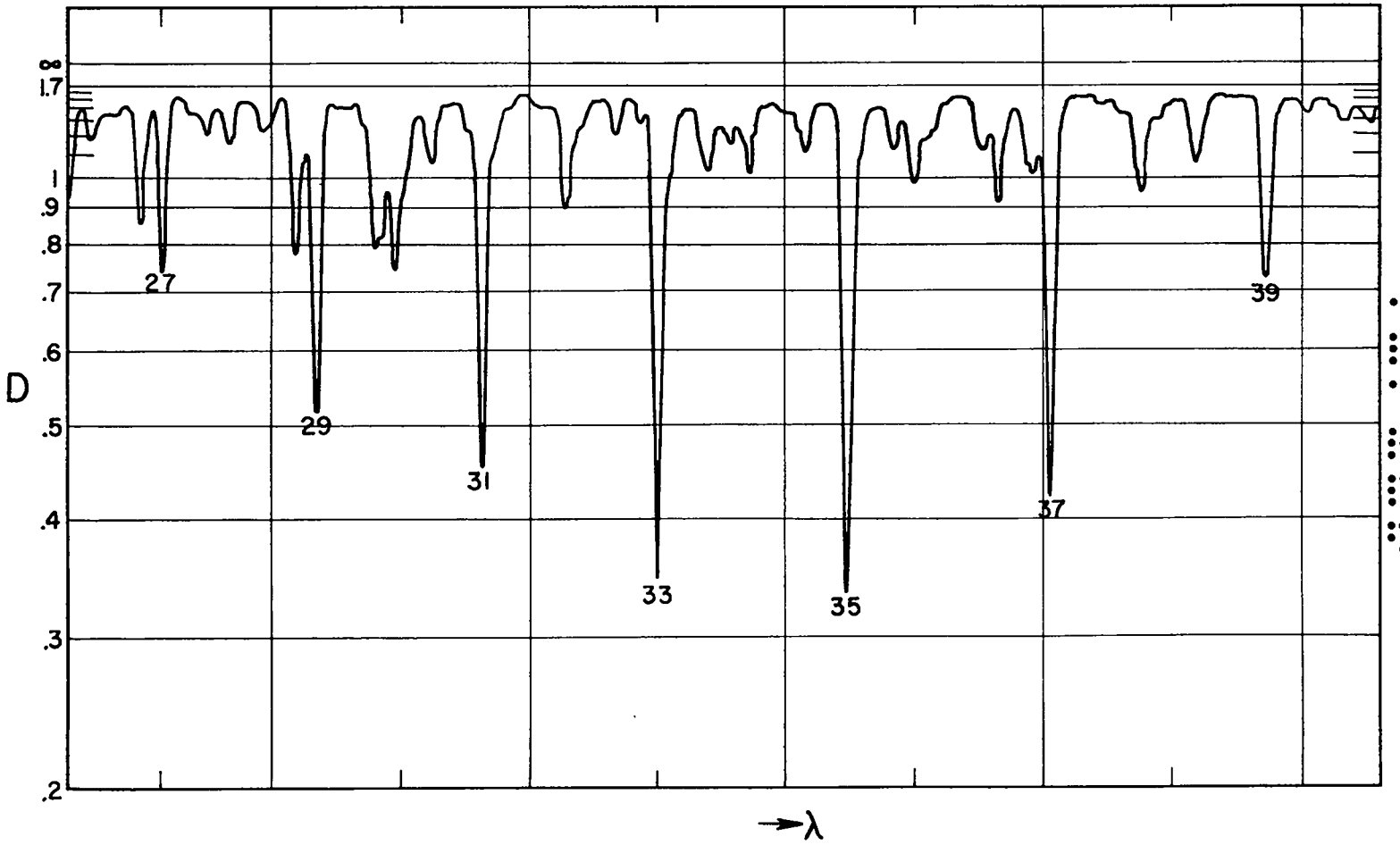

Fig. 15. Absorption by hot oxygen in the 0-14 band for the shot of October 28, 1951. Light was from the second maximum. (From LA-1329)

for the lines of the 0-14 band shown in Figure 13 is K = 31. The maximum of intensities on Figure 15 is near K = 35. This corresponds to a rotational temperature of about 4000°K. This evidence indicates that the air around the fireball during the later period is very hot and presumably near equilibrium.

On Figure 15 the intensities appear fairly regular in the vicinity of the maximum. On some other spectra the intensities are very erratic. There is evidence that this is not primarily due to neighboring iron lines. The NO_2 absorption may be responsible, but this question cannot be cleared up until the laboratory NO_2 absorption is better known. Superimposed absorption will make certain lines appear stronger than they really are. Other absorption lines that come out considerably weaker than would be expected from their neighbors may be caused by superimposed emission lines. More laboratory experiments are needed to clear up the nature of this interference.

4.4 Time Variation of O_2 Absorption

The first maximum, low rotational temperature, bands are practically impossible to see in low resolution spectroscopy. However, the high rotational temperature or second maximum bands are very pronounced. Absorption coefficients for these bands from laboratory experiments are not available yet. It is, therefore, impossible to make quantitative measurements of the amount of excited O_2 in the optical path. However, it was possible to measure the absorption in the bands, and measurements

have been completed on the 0-15, 0-16, and 1-19 bands with wavelengths at 3516, 3673, and 4096 A respectively. Figures 16 and 17 show the absorption in these three bands as a function of time for two near nominal size bombs. The data cover the time interval from a few milliseconds past the minimum to well past the second maximum. There appears to be a tendency for peak absorption at times between 50 and 100 msec, i.e., somewhat before the second maximum.

4.5 Total Time Spectra

During the 1951 tests in the Pacific high dispersion spectra were recorded in which the spectrographwas exposed to the light from the fireball all the time. Figure 18 shows the spectra in the interval 3200 A to 3800 A recorded during the shot of April 8, 1951. The yield of this device was approximately four times nominal size. These spectra are characteristic of the second maximum because as already mentioned only about one percent of a bomb's total radiation comes out before the minimum. In Figure 18 the 0-14 band is shown in its entirety, a 300 A interval, up to K = 79. The maximum intensity seems to be at K = 33.

Schumann-Runge bands and iron lines are the most prominent features of these high dispersion spectra. It is characteristic of these shots that not much iron absorption is seen below 4000 A. Also lines due to water, OH, and other metals are seen. There was an indication of weak NO_2 absorption on the original plate but it does not show on the microphotometer trace.

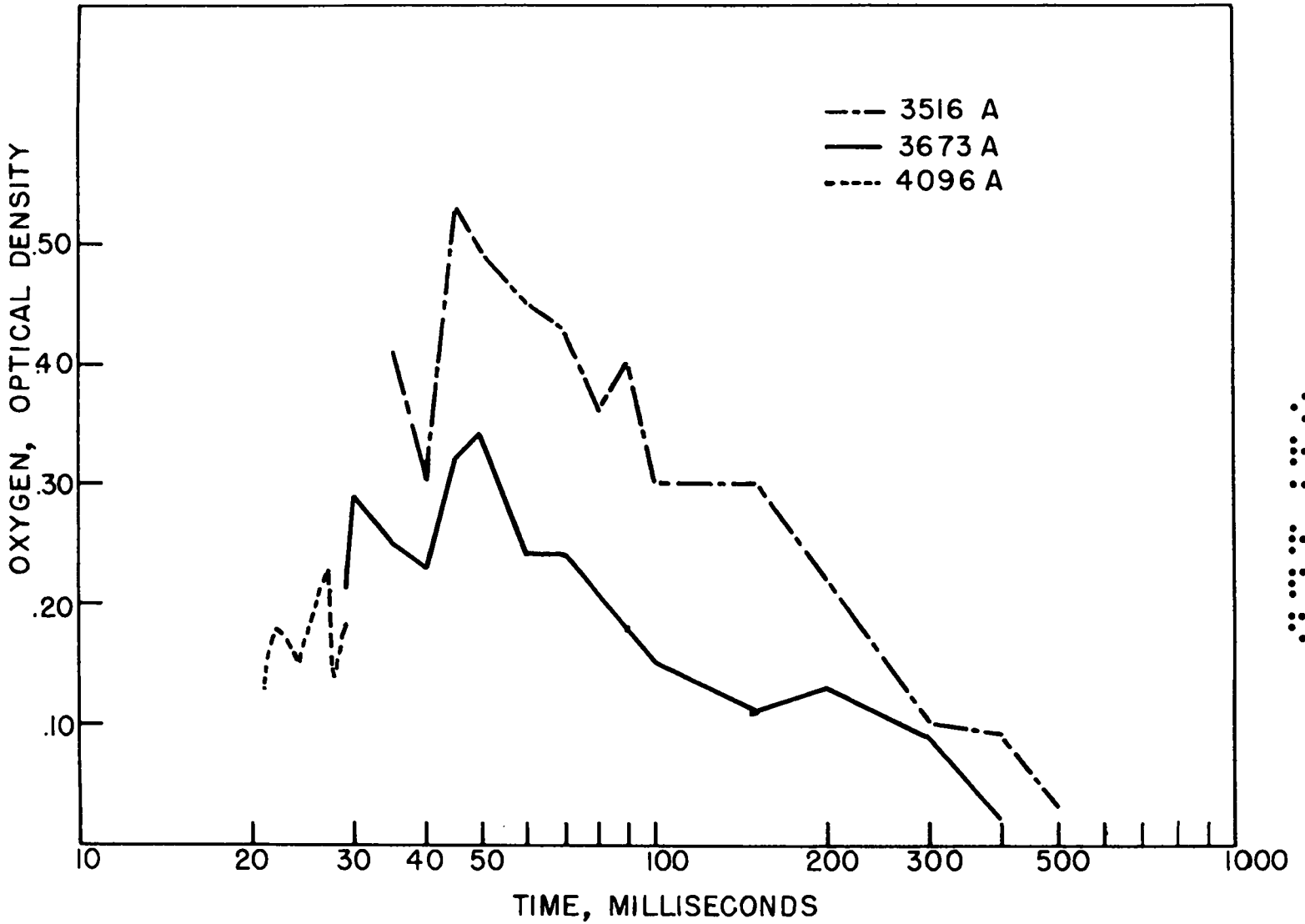

Fig. 16. Curves of optical density vs time for three band systems of oxygen for the shot of March 17, 1953 (from NRL-4337).

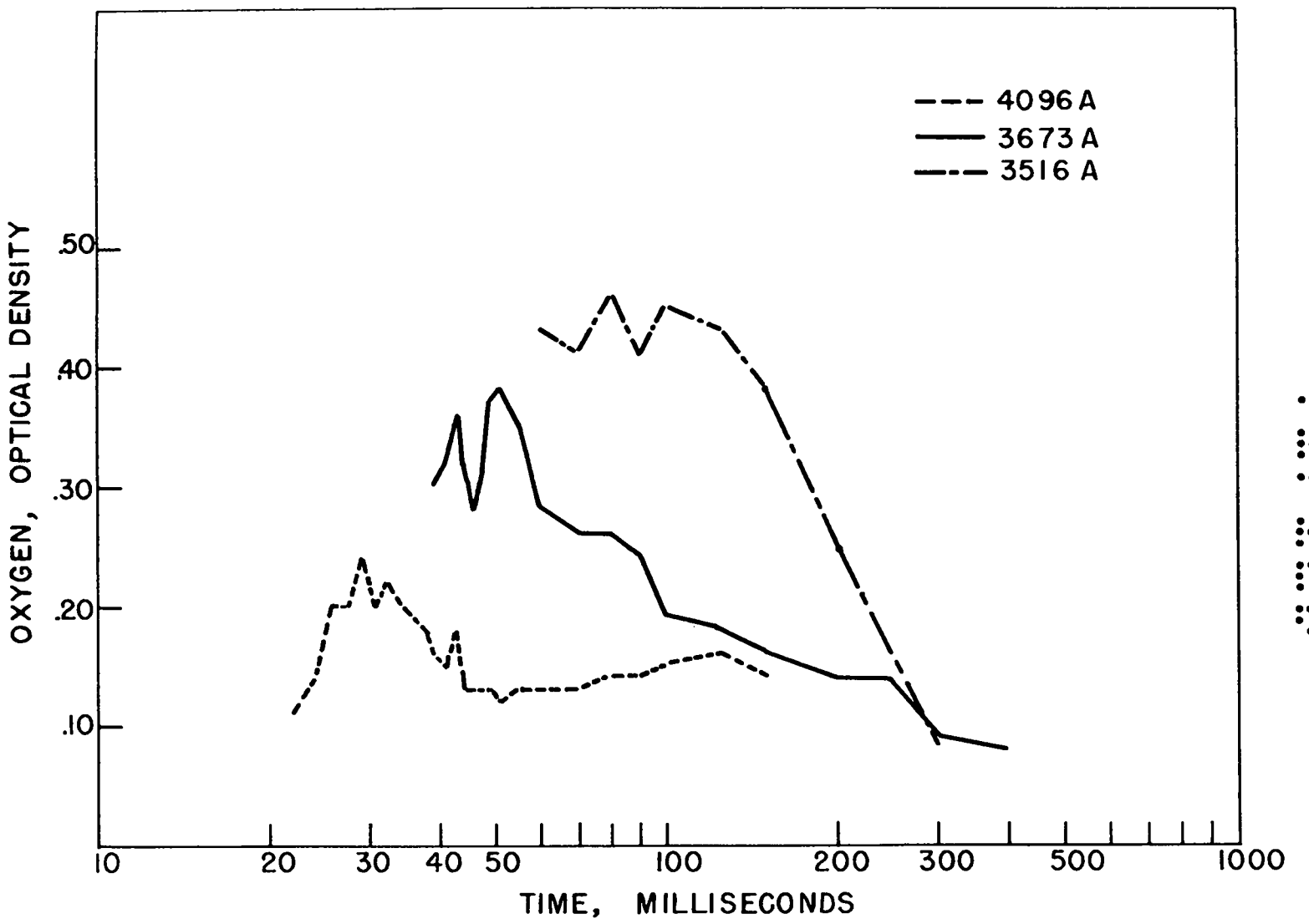

Fig. 17. Curves of optical density vs time for three band systems of oxygen for the shot of April 18, 1953 (from NRL-4337).

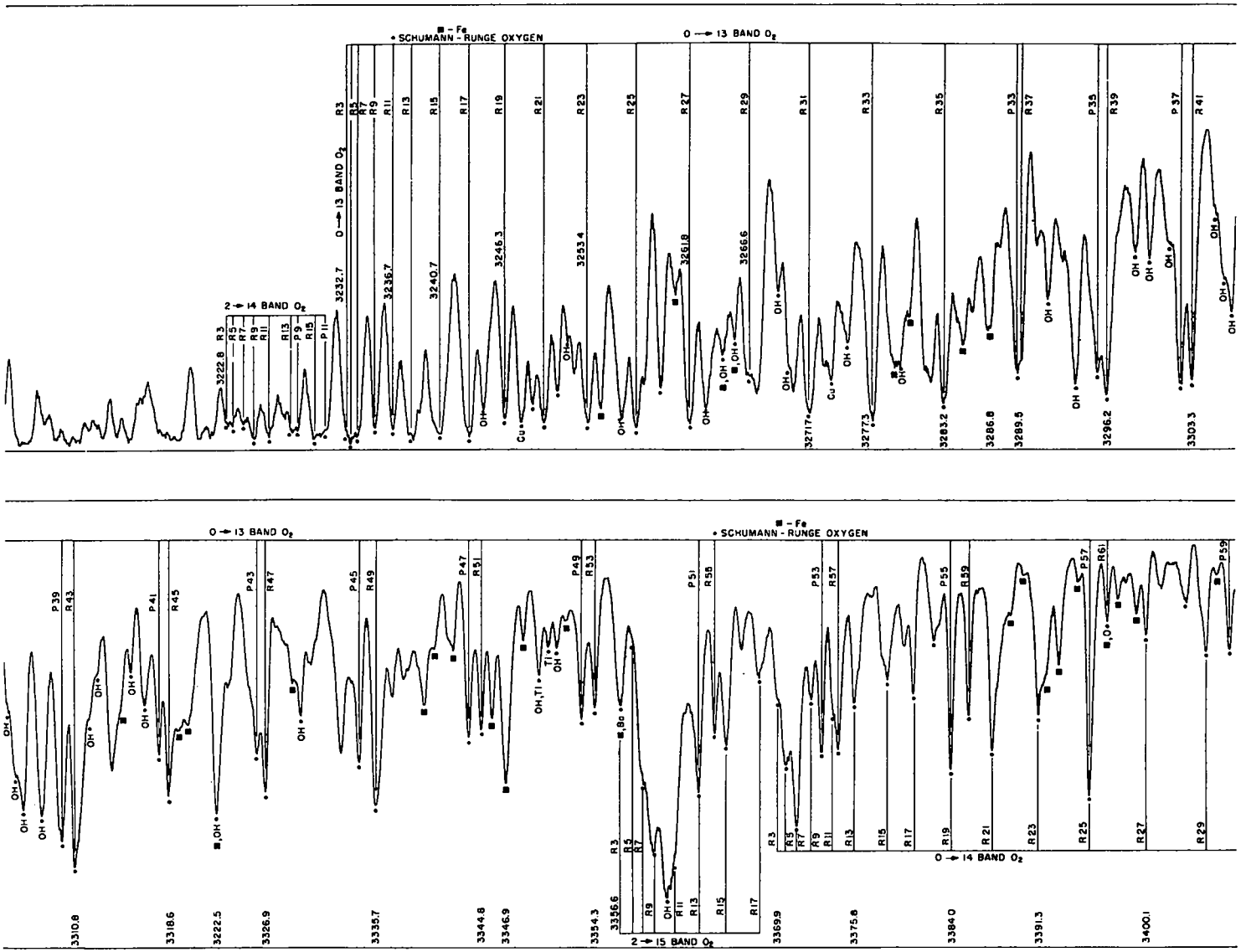

Fig. 18. Total time high dispersion spectra for the Pacific shot of April 18, 1951, showing the spectral region 3200 to 3800 A (from NRL-4434). Figure continues on next two pages.

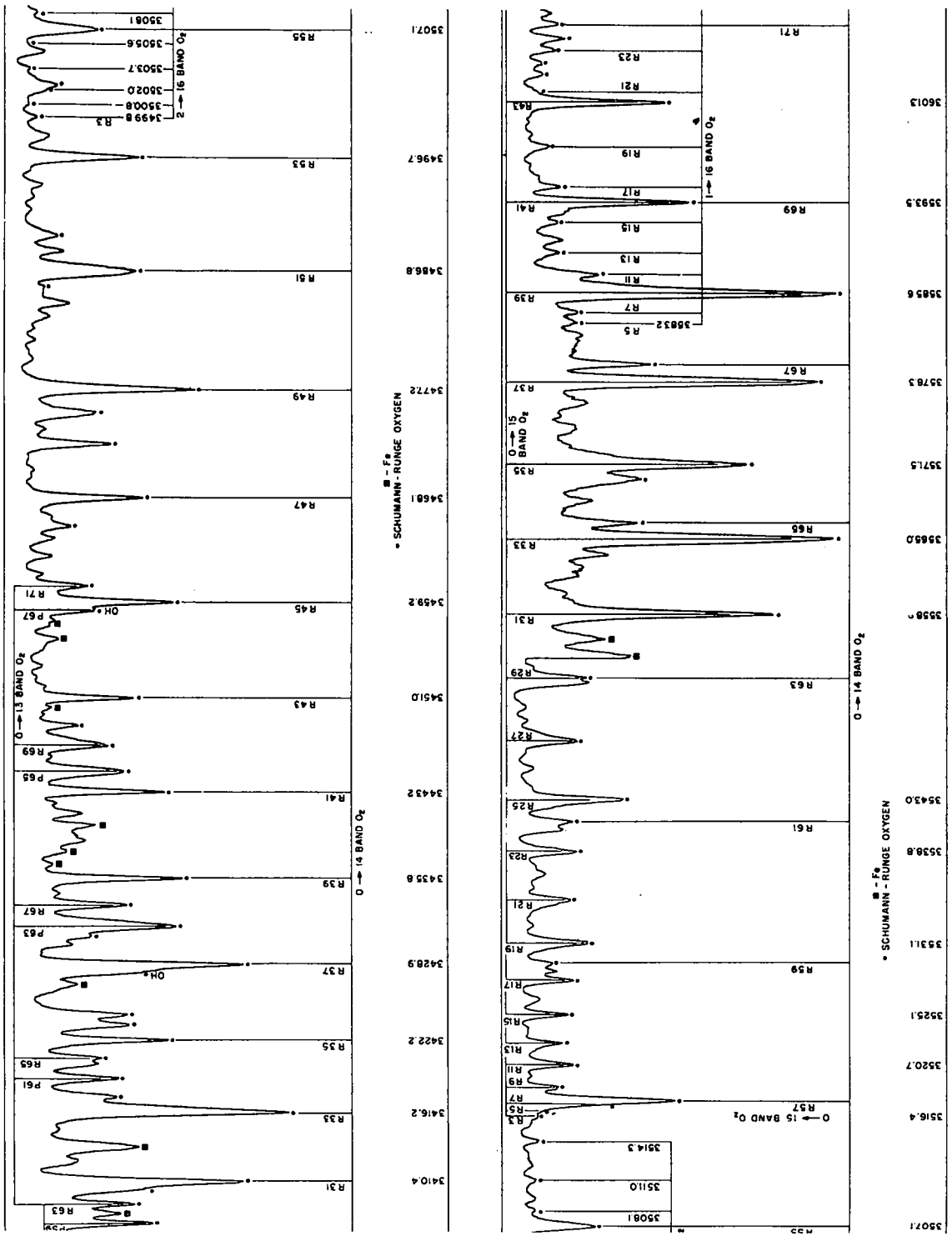

Fig. 18 (second page)

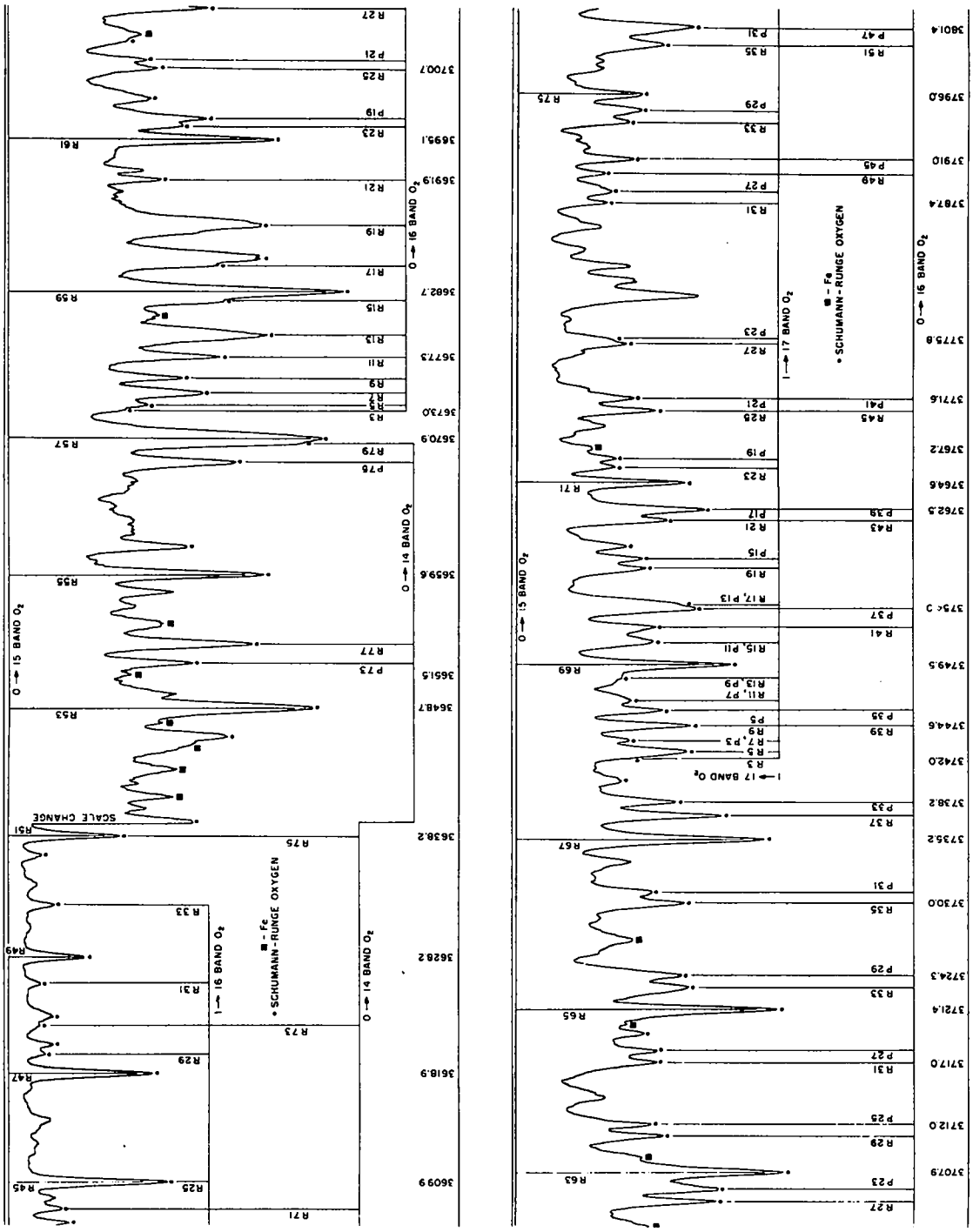

Fig. 18 (third page)

4.6 Line Widths

Although Schumann-Runge bands are strong on the low dispersion spectra such as Figs. 7 and 8, it is clear that these bands absorb only a small fraction of the continuous radiation from the fireball. A look at the high dispersion spectra such as Figs. 15 or 18 shows the reason. The rotational lines in a band are quite narrow. In Fig. 15 the most intense lines do not take out more than a few percent (maybe 5%) of the continuous radiation. Thus the band absorption is quite weak compared to the continuous Schumann-Rung absorption of wavelengths below 2200 A or so. This observation is of importance in considering the possible radiation from the hot air behind the shock front of a high velocity missile. Since the absorption lines of the Schumann-Runge bands are narrow, the emission lines will also be narrow. Hence there is no reason to expect a large amount of radiation from oxygen molecules excited to the $B^3\Sigma$ electronic state behind the shock front.* The continuous radiation, however, may be very important.

The observed line widths are due principally to four causes which may all be present simultaneously: instrument width, Doppler width, pressure broadening, and field broadening.

*It should be remembered, however, that the absorption of the radiation emitted near the second maximum is due to the relatively cold air between the fireball and shock wave, whose temperature is certainly less than 6000°K. Temperatures up to 8000°K may occur near the stagnation point in front of a re-entering missile, and at higher temperatures more rotational and vibrational levels are available, leading to a fuller coverage of the spectrum with lines.

The instrument width results from the finite resolving power of any spectrograph. This finite width depends on the particular instrument used and on the state of adjustment as well as on the slit width. Most of the spectra shown in this report were taken with a Baird 2-meter spectrograph, which has a theoretical resolving power of about 60,000. With narrow slits and good adjustment the instrument width at 4000 A is of the order of magnitude of 0.07 A. The instrument width shape depends very much on the particular instrument and its imperfections.

The Doppler width is caused by the temperature motion of the gas. The shape of a line with Doppler broadening is:

$$I(\nu) = \text{constant } e^{-\beta \frac{c^2}{\nu_o^2} (\nu - \nu_o)^2}$$

where $\beta = A/2RT$, A is the molecular weight, R the universal gas constant, and T the absolute temperature. The half-width in Angstrom units is

$$2 W_D = 2 \frac{\lambda}{c} \sqrt{\frac{2RT}{A} \ln 2} = 1.67 \frac{\lambda}{c} \sqrt{\frac{2RT}{A}}$$

For O_2 (A = 32) at 5000°K, the half-width is

$$2 W_D = 8.95 \times 10^{-6} \lambda$$

or at 4000 A

$$2 W_D \cong 0.04 \text{ A}$$

This figure is smaller than the instrument width. Temperature measurements through the Doppler width are therefore practicable only at much higher temperatures or with instruments of higher resolving power. Even then the Doppler width would have a meaning only if pressure and other broadenings are not predominant.

Pressure broadening, also known as collision damping, results from the collision of two atoms or molecules interfering with the radiation process. If two molecules collide elastically while one is emitting or absorbing radiation, the phase and amplitude of the radiation have a chance of undergoing a considerable change. The resulting spectral line is usually broadened asymmetrically and shifted toward the long wavelength side.[13] A simple classical calculation of this broadening[14] starts with the assumption that the mean time between collisions is large compared with the collision time, and that the collision time is considerably greater than the period of the radiation. For normal temperatures and normal effective cross sections the collision time is of the order of 10^{-13} seconds, and the period of visible light is about 10^{-15} seconds. This calculation gives a resonance shape

$$I(\nu) = \text{constant} \frac{1}{4\pi^2(\nu - \nu_o)^2 + (1/\tau_o)^2}$$

[13] O. Oldenberg, Z. Physik 47, 184 (1948); 55, 1 (1929); W.M. Preston, Phys. Rev. 51, 298 (1937).

[14] H. E. White, Introduction to Atomic Spectra, pp. 427-434, McGraw-Hill Book Co., Inc., New York, 1934.

where τ_o is the mean flight time between collisions. The half-width of this expression is

$$\delta^{\nu} = \frac{1}{\pi \tau_o}$$

The value of τ_o is the ratio of the mean free path given by the kinetic theory of gases to the average velocity of the molecules. This treatment gives the half-width as

$$2\,W_P = \frac{\lambda^2}{c}\,\frac{N\rho}{A}\,\pi d_{opt}^2\,\sqrt{2}\,\sqrt{\frac{8RT}{\pi A}} = \frac{\lambda^2}{c}\,4N\,d_{opt}^2\,\rho\,\sqrt{\frac{RT}{\pi A^3}}$$

where N is Avogadro's number, A the molecular weight, ρ the density, and d_{opt} the collision diameter of the optical cross section. The value of d_{opt} is some two or three times larger than the collision diameter of the usual kinetic cross section. For oxygen it is approximately 8 A. Hence for oxygen

$$2\,W_P \cong 0.01\;\lambda^2\,(\frac{\rho}{\rho_o})\,\sqrt{T}$$

where ρ_o is normal atomospheric density and ρ is the actual density. At 4000 A this estimate of the half-width for T = 5000°K in Angstrom units is

$$2\,W_P \cong 0.1\,(\frac{\rho}{\rho_o})$$

Even at normal atmospheric density this estimate is of the order or larger than either the instrument width or Doppler width.

The width of the prominent oxygen lines in the high dispersion spectrum shown in Fig. 18 is about 0.7 A. Considering that the density of air behind the shock front may be several times normal atmospheric density, it seems that pressure broadening could account for this observed width.

The line shape and half-width expressions given above for pressure broadening should be understood as rough estimates from a crude theory. At present there is no good quantum mechanical treatment of the pressure broadening and shift. The effect depends not only on the number of collisions but also on the different kinds of molecules in air that can collide with and disrupt the radiation process in O_2.

If the atoms that absorb or radiate are subject to strong electric fields, the Stark effect will shift the lines, and since in a vapor the intensity of the fields is distributed at random, a widening will result. This widening may be asymmetric because in all substances except atomic hydrogen, the Stark effect is quadratic in the field. The ion density would be the quantity chiefly determining Stark broadening. The field broadening cannot be strictly separated from collision broadening because the highest fields are experienced during the collision process.

Through the motion of large number of ions or electrons, macroscopic electric currents may be set up which might result in magnetic fields that are constant over considerable areas and produce an actual line splitting due to Zeeman effect. No such splitting has ever been observed in spectra from nuclear explosions.

5. OBSERVATION OF NO_2

5.1 Formation of NO_2 Behind the Shock Front

The formation of considerable quantities of NO_2 behind the shock front just before the time of the minimum is important because of its effect in darkening the fireball and strengthening the blast.

Curtiss and Hirschfelder[15] have calculated the equilibrium concentration of NO_2 in air for temperatures below 5000°K. The air has very little NO_2 before it enters the shock and so some time is required to form NO_2 after the air has been heated by the shock. Formation of NO_2 in heated air under laboratory conditions has been studied by Daniels.[16] Presumably the mechanism for formation is in two steps

(a) $N_2 + O_2 \longrightarrow 2NO$

(b) $2NO + O_2 \longrightarrow 2NO_2$

---

[15] Curtiss and Hirschfelder, Thermodynamic Properties of Air, University of Wisconsin Naval Research Laboratory, 1948.

[16] Private communication by Prof. Farrington Daniels. He gives the reaction rate constants for $NO_2 + O_2 \underset{k_b}{\overset{k_j}{\rightleftharpoons}} 2NO$ as

$$k_j = 10^{8.5} \exp - (45{,}280/T) \text{ (atm sec)}^{-1}$$

$$k_b = 10^{9} \exp - (34{,}000/T) \text{ (atm sec)}^{-1}$$

Reaction (b) is extremely fast at all temperatures above 600° and will always maintain equilibrium between NO, O_2, and NO_2. The rate of reaction (a) is strongly temperature dependent and so effectively one can say that it takes place above a certain temperature and does not occur below this temperature. Below 2000° there is a negligible amount of NO_2. The NO_2 zone is therefore limited to the air which was initially within the radius for which the shock temperature is more than 2000°, about 120 meters for a nominal bomb.

After the time of the minimum the shock front is no longer hot enough to form NO_2; however, there is still quite a bit of NO_2 behind the shock around the surface of the fireball, in the material which originally went through the hot shock.

5.2 Analysis of Spectra to Obtain Amounts of NO_2

During the 1953 tests in Nevada it was attempted to get information on the variation with time of the effective NO_2 concentration between the fireball and the spectrograph. Useful spectra were obtained on seven shots. Absorption in eight NO_2 bands was determined as a function of time for each of the useful spectra. These absorption values were converted through published absorption coefficients into quantity of NO_2 expressed as thickness in millimeters, at standard temperature and pressure. The results are plotted as a function of time.

Figure 19 is a composite print showing laboratory ozone and NO_2 absorption spectra compared with the first seven milliseconds of

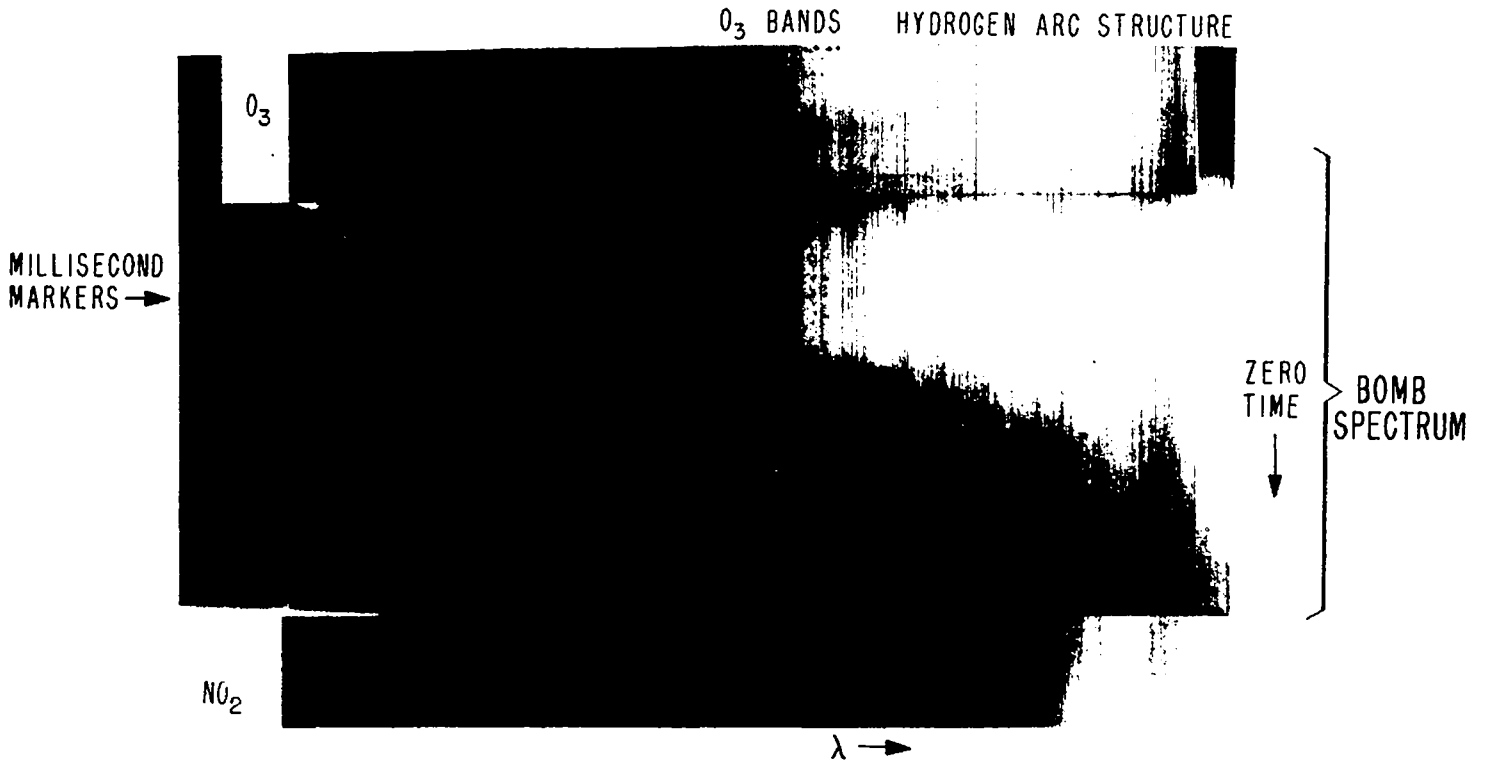

Fig. 19. Composite print showing laboratory ozone and NO_2 absorption spectra compared with the spectrum of the shot of March 17, 1953, for the first 7 msec (from NRL-4322).

bomb spectra. The presence of ozone and NO_2 in the bomb spectra is clearly indicated. Figure 20 is a typical microphotometer trace showing the NO_2 bands in the spectrum of the shot of May 19 at about seven milliseconds. The eight bands marked were the ones used in the analysis.

The absorption coefficients used in reducing the NO_2 data are those of Hall and Blacet,[17] whose absorption curve is shown in Figure 21. Examination of this curve shows many pronounced absorption maxima superposed on a strong continuum. In the work reported in this section eight of the more prominent maxima were selected, corresponding to the eight bands marked on Fig. 20. The results presented are the average of eight independent measurements for each data point.

In making the calculations, it was convenient to divide the absorption coefficient into two parts, one due to the continuum and the other due to band absorption. The coefficients used were the differential coefficients of the bands relative to the continuum. These differential coefficients, listed in Table 3, were obtained by subtracting the coefficients of the continuum envelope from the coefficients at the centers for the various bands.

[17] T. C. Hall, Jr. and W. Blacet, J. Chem. Phys. 20, 1745 (1952).

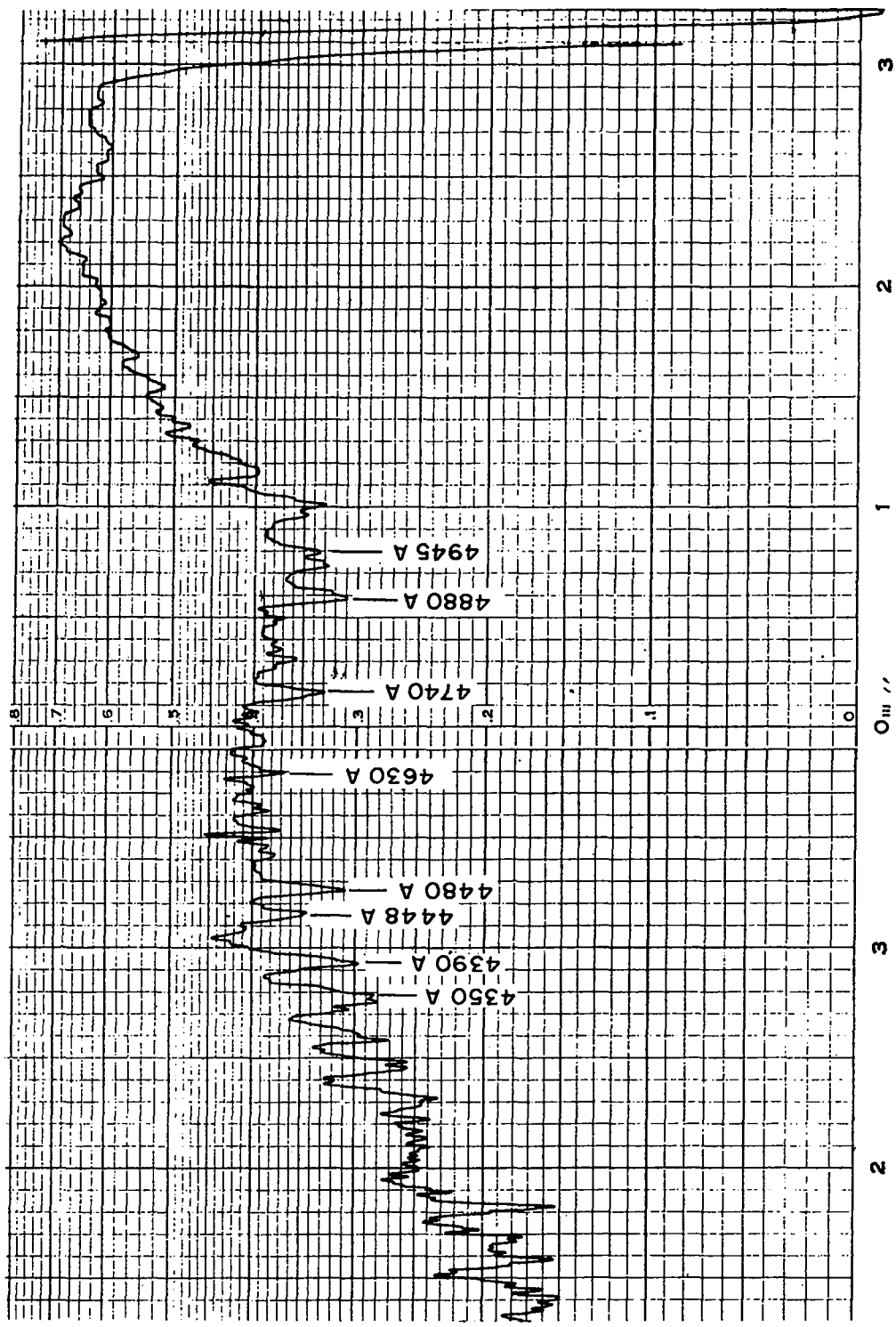

Fig. 20. Microphotometer trace showing NO_2 bands studied (from NRL-4322).

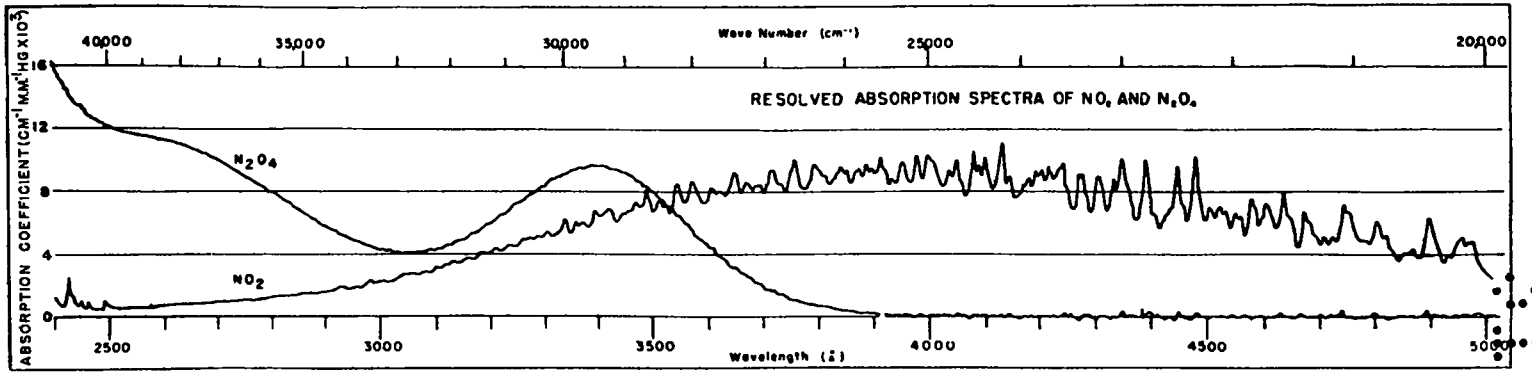

Fig. 21. Absorption coefficient vs wavelength and wave number for NO_2 and N_2O_4 measured at 25°C. The quantity plotted here is $(1/P\ell)\ \log_{10}\ (I_o/I)$. The absorption coefficient for the usual exponential transmission law $I_\nu = I_{\nu o}\ e^{-\alpha \nu \ell}$ is

$$\alpha_\nu = \frac{1}{\log_{10} e}\ \left(\frac{1}{P\ell}\ \log_{10}\ \frac{I_o}{I}\right)_\nu$$

(From NRL-4322; originally from the article of Hall and Blacet in J. Chem. Phys. 20, p. 1745.)

TABLE 3

WAVELENGTHS AND DIFFERENTIAL ABSORPTION

COEFFICIENTS FOR NO_2 BANDS

Wavelength, A	Differential Absorption Coefficient, cm^{-1} $(mm\ Hg)^{-1}$
4350	1.8×10^{-3}
4390	2.0
4448	1.8
4480	2.0
4630	1.7
4740	1.6
4880	1.2
4945	1.2

The intensity of band absorption at any time was obtained from the microphotometer trace of the picture taken at that time by comparing the intensity of the band to the intensity of the continuous background at the same wavelength (see Fig. 20). Intensities were derived from the microphotometer traces through the characteristic curves of the emulsion.

5.3 Time Variation of NO_2 Concentration

Figure 22 shows a typical time curve for the amount of NO_2 between the fireball and the observer obtained by the means described in the preceding paragraphs. The shot of March 17, 1953, for which this curve was taken, was slightly below nominal size. The optical system

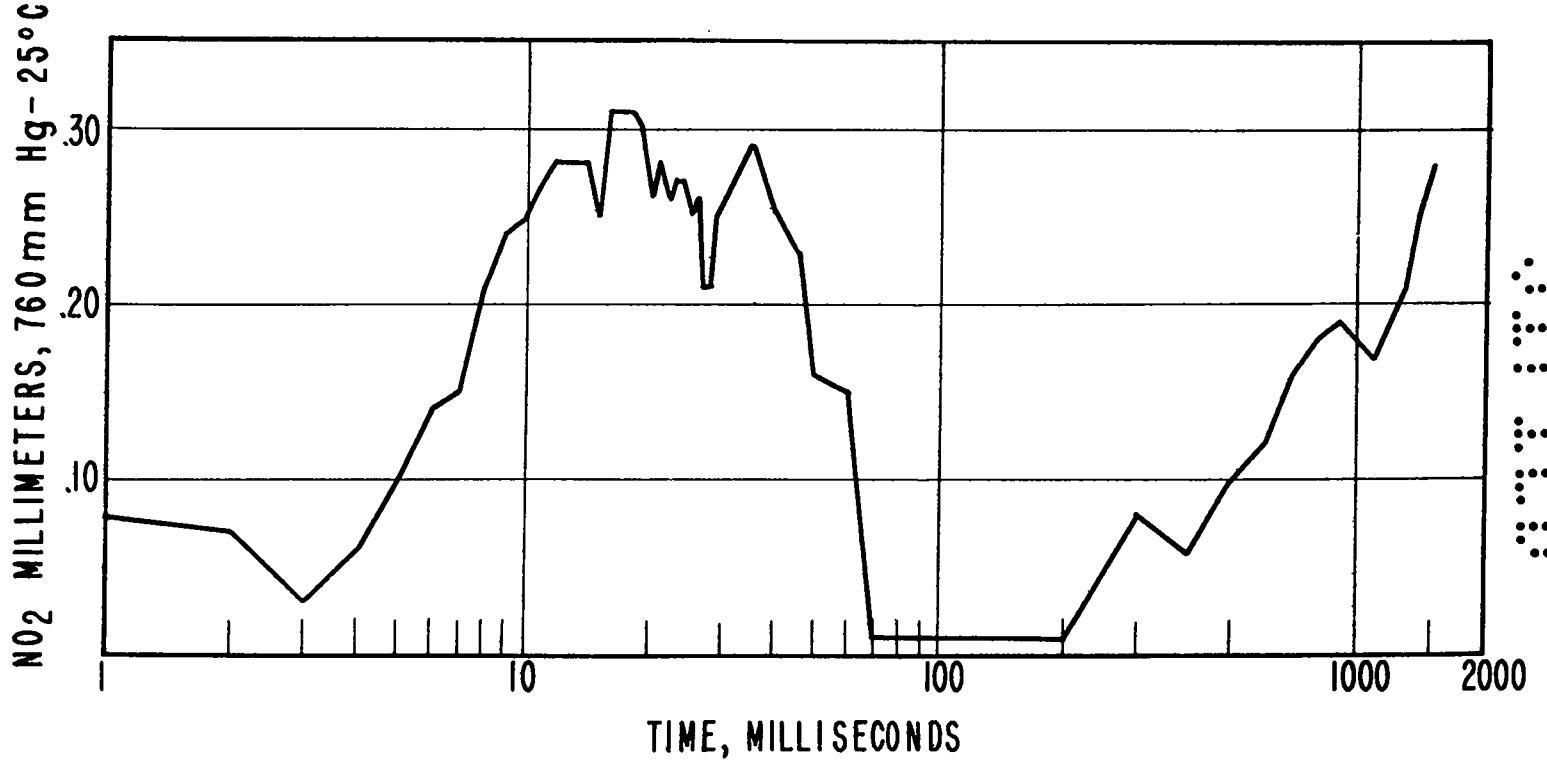

Fig. 22. Equivalent thickness of NO_2 between spectrograph and bomb in millimeters, as a function of time for the shot of March 17, 1953 (from NRL-4322).

for taking 100 μsec exposures every 1.7 msec did not function for this shot. However, the spectrograph was pointed toward ground zero and streak spectra were obtained for 1500 msec. The time resolution is 3 msec.

The NO_2 content is seen to vary from 0.03 mm (thickness of an equivalent layer at normal temperature and pressure) at 3 msec to a peak of 0.31 mm at about 17 msec and then gradually decay to a trace (less than 0.01 mm) at 70 msec. The first peak between 0 and 3 msec is real. A trace amount of NO_2 existed from 70 to 250 msec, i.e., during the period of the second maximum. From 250 msec on there was a gradual increase to about 0.28 mm at 1500 msec, which was the final measurable spectrum. This increase was not found on any other shot.

The time curves obtained from five different shots show much the same features as Fig. 22. Table 4 gives the initial concentration, the maximum concentration, and the duration of the maximum (defined by the times when the concentration was 2/3 of the maximum).

TABLE 4

OBSERVED NO_2 CONCENTRATIONS

Date of Shot, 1953	Initial Concentration, mm at NTP	Maximum Concentration, mm at NTP	Duration of Maximum, msec
March 17	0.08	0.31	40
March 24	0.00	0.24	33
April 18	0.21	0.44	38
April 25	0.15	0.38	48
May 19	0.07	0.47	46

The shots listed in Table 4 range from slightly less than nominal size to more than double nominal size (shot of April 25). The shot of March 24, a little more than nominal size, is interesting in that the early peak concentration of NO_2 observed in the other shots is not present. Also the peak concentration is smaller and the duration of this peak is shorter than for the other shots. The shot of March 17 (Fig. 22) is unique in showing an increase of NO_2 after 250 msec. On the other curves no trace of NO_2 was observed after 250 msec.

Two shots in this series were extremely small nuclear explosions, of the order of one hundredth the yield of a nominal bomb. The spectra were unusual in that little evidence of the minimum was seen. Using the scaling law one would expect the minimum at $(1/100)^{1/3}$ 12 = 2.6 msec. Some of the color temperature curves for these shots show a minimum at about 3.5 msec; and some show no minimum at all. The second maximum, if distinguishable at all from the first maximum, is of very short duration. The spectra of these small shots are also unusual in that no evidence of absorption by NO_2, O_3, or HNO_2 could be seen. It may be that these substances are not formed in sufficient concentration in front of the fireball to show up in absorption.

The work reported above indicates that the amount of NO_2 between the fireball surface and a distant observer varies markedly in time. The observed amount seems to peak to a maximum of a few tenths of a millimeter at about the time of the minimum and stay at this amount for another 40 msec or so. It should be kept in mind that these results

were obtained by using published absorption coefficients valid at about 300°K. Any possible temperature effects have been ignored for two substantial reasons: the variation with temperature of the absorption coefficient of NO_2 is unknown, and the temperature of NO_2 around the fireball is not known at the present time.

The absorption coefficient of NO_2 through the range 4500 A to 7000 A for T = 300° has been measured by Dixon.[18] His measurements, supplementing those of Hall and Blacet which stop at 5000 A, indicate that the absorption coefficient decreases rapidly toward the red end of the visible spectrum. There are indications that at much higher temperatures this is not the case. The addition of NO_2 to some flames changes the flame color to a yellow-green. This is attributed to the radiative recombination $NO + O \longrightarrow NO_2 + h\nu$ and is used as a qualitative test for the presence of atomic oxygen. This radiation covers the spectral region from 5000 to 6500 A. Unfortunately the mechanism is quite complex since it does not seem to involve the ground state of NO_2. The same radiation is also found to be present in the afterglow of an air discharge.[19]

From Fig. 21 the maximum NO_2 absorption at 300°K is seen to occur at about 4000 A

---

[18] J. K Dixon, J. Chem. Phys. 8, 157 (1940).

[19] A. G. Gaydon, Spectroscopy and Combustion Theory, p. 101, Chapman & Hall, Ltd., London, 1948.

$$\alpha_{max} = \frac{1}{P\ell} \log_e \frac{I_o}{I} = 2.1 \times 10^{-2} \text{ cm}^{-1} \text{ (mm Hg)}^{-1}$$

The maximum concentration of NO_2 in air at normal density and at equilibrium occurs at about 4000° and is about 0.8×10^{-4}. Such a concentration might occur behind the shock front of a missile. However, the thickness of air with this concentration of NO_2 that radiation must pass through in order that its intensity be reduced by 1/e is 800 cm. Actually the thickness of hot air between the shock front and a missile is about five centimeters. Hence radiation from NO_2 is negligible, if the room temperature absorption coefficients are approximately correct at 4000°. However, the flame tests described by Gaydon indicate that the absorption may be very large at 6000 A for NO_2 at high temperatures in which case NO_2 may be very important behind a missile shock.

6. OTHER STRANGE MOLECULES

6.1 HNO_2

6.1.1 Formation of HNO_2

The most conspicuous feature in early-time, low-dispersion spectra, such as Figs. 4 and 5, is a series of bands between 3200 and 3845 A. These bands have been observed by several investigators.[20, 21] There was for a long time a controversy as to the molecule which was

[20] E. H. Melvin and O.R. Wulf, J. Chem. Phys. 3, 755 (1935).

[21] E. H. Newitt and W. A. Bone, Proc. Roy. Soc. London 115, 41 (1927); E. H. Newitt and L. E. Outridge, J. Chem. Phys. 6, 752 (1938).

responsible for these bands. Newitt and Bone and Newitt and Outridge had observed similar bands in the spectrum of a CO-N O-NO explosion which they attributed to NO_2 under special conditions, while Melvin and Wulf attributed the absorption to HNO_2. The matter appears to have been settled recently and there seems to be little doubt that the molecule is HNO_2.

The bands are shown in Fig. 23, which was taken for a large shot in the Pacific on May 9, 1951. They are diffuse and broad, indicating predissociation in the upper state of the molecule. They are inconspicuous under high dispersion. The 3539 A band overlaps the 0-15 O_2 band and the 3680 A band the 2-16 O_2 band (Fig. 14).

The chief laboratory evidence concerning these bands comes from the work of Melvin and Wulf who found that the bands occur in mixtures of H_2O, NO, and NO_2. They showed that all three constituents were necessary for the bands to occur and attributed them to the molecule HNO_2. Newitt and Outridge believed they had found evidence that H_2O was unessential for formation of the bands and attributed them to NO_2. It is quite possible[22] that the bands they observed were not those of Melvin and Wulf.

The matter was definitely settled by Porter[23] who showed that when H_2O in the mixture was replaced by D_2O there was a definite shift of the bands, showing that the molecule must contain hydrogen. Jones,

---

[22] H. W. Thompson, J. Chem. Phys. 7, 136 (1939).
[23] G. Porter, J. Chem. Phys. 19, 1278 (1951).

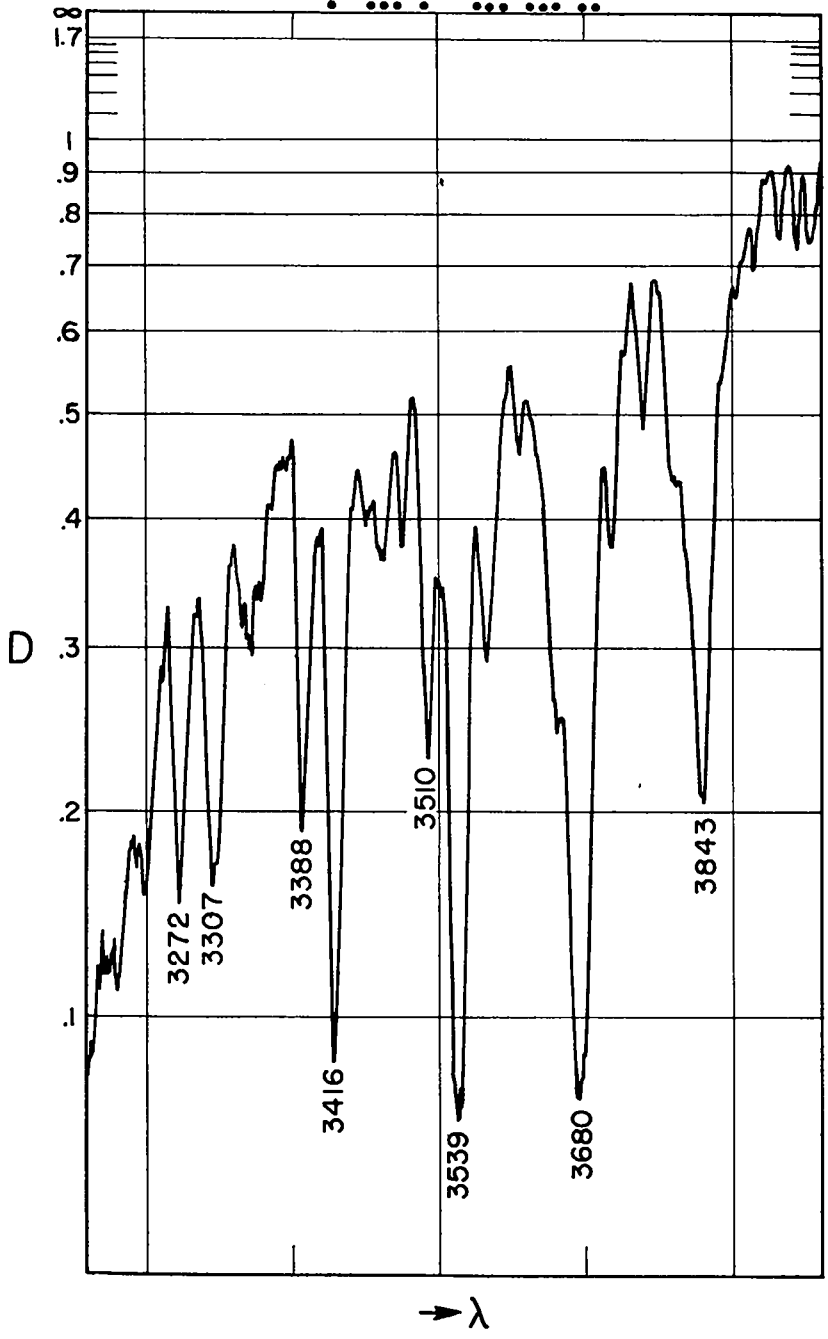

Fig. 23. Absorption bands of HNO_2 for the Pacific shot of May 9, 1951. Note how much more pronounced the bands are for this shot than for the Nevada shot shown in Figs. 4 and 5. (From LA-1329)

Badger, and Moore[24] investigated the infrared spectrum of HNO_2 and DNO_2 and obtained clues to the structure of the molecule, while Wayne and Yost[25] investigated the kinetics of the reaction between NO, NO_2, and H_2O. They found that with a typical set of pressures, equilibrium establishes itself within a few hundredths of a second. They estimate that at 25°C with partial pressures of 570 mm of NO, 15 mm of NO_2, and the saturation pressure of H_2O at 25°C, they have 18 mm of gaseous HNO_2. They attribute the formation of this molecule to triple collisions, according to the formula

$$NO + NO_2 + H_2O \longrightarrow 2HNO_2$$

but leave other possibilities open. The molecules must be very unstable. When the temperature is raised, the absorption bands become weaker and have practically disappeared at 100°C.

While there seems little doubt now that the bands must be ascribed to HNO_2, much remains to be cleared up about the mechanism of formation. In any bomb spectrum the bands are present from the earliest moments that the continuous background is observed. If the mechanism that Wayne and Yost studied in a mixture of NO, NO_2, and H_2O at room temperature is the one responsible in the spectrum of the fireball, we must assume that in a few microseconds enough NO and NO_2 have been formed to give, through triple collisions that also involve H_2O

---

[24] L. L. Jones, R. M. Badger, G. E. Moore, J. Chem. Phys. 19, 1599 (1951).

[25] L. G. Wayne and D. M. Yost, J. Chem. Phys. 19, 41 (1941).

molecules, an appreciable amount of HNO_2. This seems very unlikely.

There is much room for additional laboratory work. It should be investigated whether excited molecules or atoms cannot provide a faster reaction, possibly one that does not require triple collisions. With the equilibrium constant of the ordinary reaction known, the absolute strength of the absorption can be measured in the laboratory with comparatively little difficulty. This would make it possible to measure the number of molecules responsible for the absorption in the fireball. While it seems now generally agreed that HNO_2 is the molecule responsible for these bands, it should be ascertained whether another combination of H, N, and O such as HNO can be definitely ruled out.

Ordinarily the bands appear with the first traces of the continuous background (Fig. 4), but this is not always true. The smallest shots show little or no absorption by HNO_2. The bands seem to decrease in intensity at the beginning, thereby strengthening the assumption that the molecules are originally formed by the action of gamma rays. The bands increase then in strength again and are very prominent near the minimum. In the later stages they seem to be inconspicuous or greatly modified. In general they seem to be stronger on plates from shots in the Pacific than on Nevada plates.

6.1.2 Time Variation of HNO_2

It was not possible to make quantitative measurements of the HNO_2 content between the observer and the fireball as was done with NO_2

because no absorption coefficients are available for the bands. However, it was possible to determine how the absorption varied as a function of time and this was done for the bands at 3543 and 3681 A. The absorption in these two bands was nearly the same and the results were averaged for each exposure. The data are plotted in Fig. 24, which shows the average optical density of the two HNO_2 bands plotted as a function of time for five shots. Optical density ranges from 0.2 to 0.3 for most of these shots. There appears to be a trend toward greater optical density for later times.

6.2 Ozone

6.2.1 Ozone Formation and Observed Spectra

There is a remarkable coincidence between the ultraviolet ends of the fireball spectrum and of the solar spectrum. Both end at about 3000 A. The end is not abrupt, but the exact termination depends on the length of the exposure.

In the solar spectrum the absorption below 3000 A has been proved to be due to ozone.[26] The ozone absorption consists of a series of very diffuse bands. They are strong below 3000 A and, with even small quantities of O_3, flow into each other so that they take out everything. Above 3000 A they can be seen in the solar spectrum superimposed on solar absorption lines. The similarity of the ultraviolet cutoff in the fireball spectrum suggests that it is due to ozone as well.

[26] A. Fowler and R. J. Strutt, Proc. Roy. Soc. London, 93, 577 (1917).

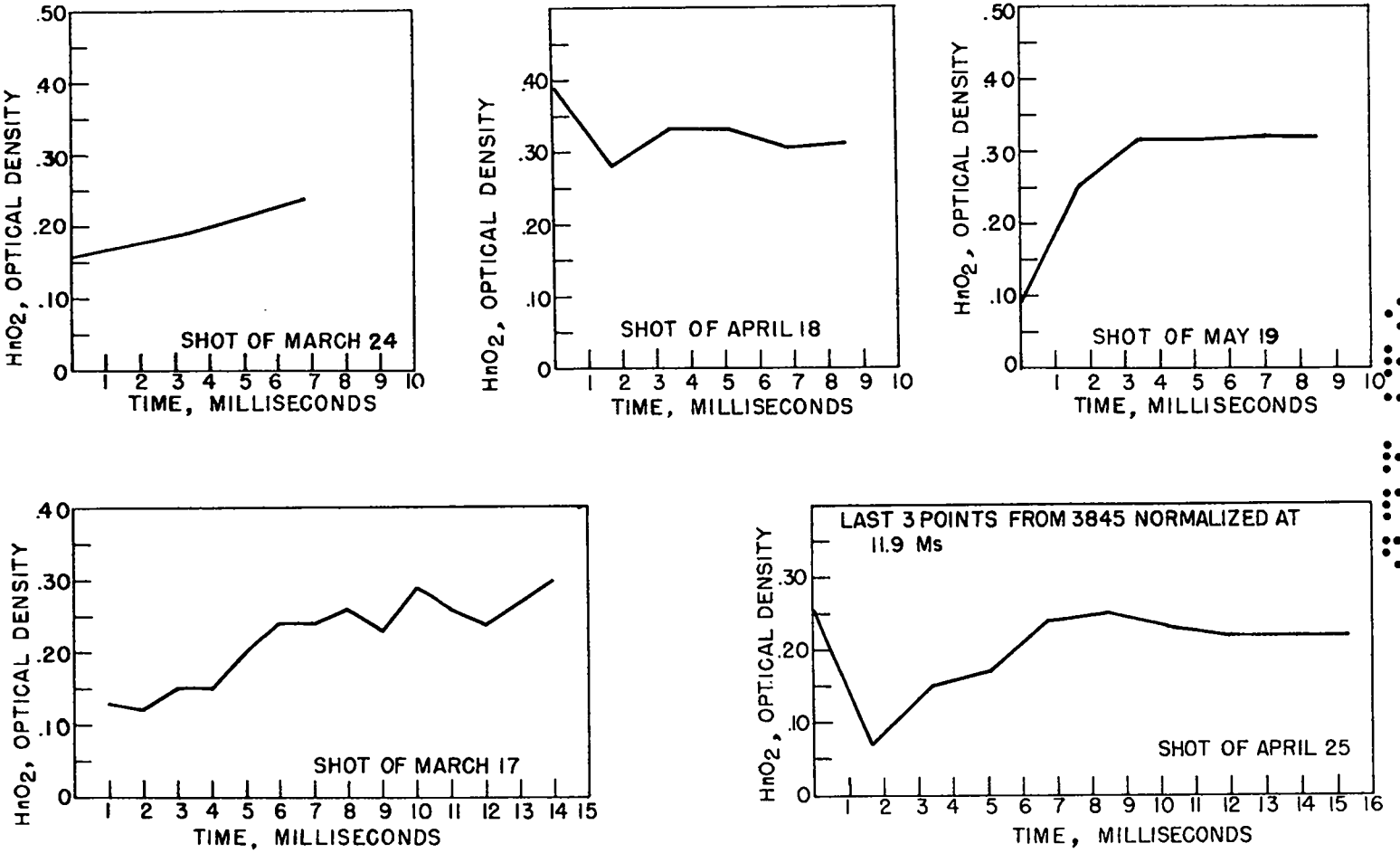

Fig. 24. Curves of HNO_2 (optical density) vs time (from NRL-4337).

Ozone has three regions of absorption which are of interest for bomb spectra. First there is a region of intense and continuous absorption below 3000 A. This absorption decreases with increasing wavelength and vanishes at about 3400 A. Superimposed on the continuum in the region 3200 to 3340 A are diffuse band structures known as the Huggins absorption bands. Another region of continuous absorption with superimposed bands is designated as the Chappuis absorption in the range from 5500 to 6000 A. The absorption in the latter region is much fainter than that in the short wavelength region.

The Huggins absorption bands are readily seen in the initial spectra of most shots. An absorption spectrum taken in the laboratory has been compared with an early time bomb spectrum in this region (Fig. 19). The presence of ozone bands is unmistakable. One can identify seven particularly strong ozone bands in the region 3200 to 3340 A. Figure 4 shows a first maximum spectrum, and Fig. 5 the spectrum from the same shot at 6.9 msec. Bands caused by ozone absorption are readily identified on these traces. The intensity of these bands compared to HNO_2 bands seems to increase after a few milliseconds, although it is difficult to estimate since they are on the slope of the continuous spectrum.

6.2.2 Time Variation of O_3 Concentration

In order to determine the quantity of ozone present, the absorption of the two bands at 3280 A and 3312 A was studied as a function of time. The spectra were microphotometered and the depth of the

absorption band relative to the surrounding continuum was translated into intensity of absorption through the characteristic curves of the film. These differential absorption measurements were interpreted in terms of equivalent thickness of ozone at normal temperature and pressure through published data on the absorption coefficients of ozone.[27] The differential attenuation coefficient for the 3280 A band was taken to be 0.072 cm^{-1} and the value for the 3312 A band was taken to be 0.056 cm^{-1}.

Figure 25 shows the equivalent thickness of ozone between the spectrograph and the bomb as a function of time for five shots of the 1953 series in Nevada. Observations were possible for only 5 to 10 msec. After this time, the ultraviolet background in the region from 3200 to 3340 A was undetectable and it was impossible to see the absorption bands of ozone. The data in Fig. 25 show that the ozone content generally varied from 1 to 2 cm. There seems to be a gradual increase in O_3 content as the minimum is approached. This is particularly noticeable for the shot of April 25, a bomb of more than double nominal yield.

Although the Huggins bands in the vicinity of 3200 A could not be seen beyond about 10 milliseconds because of the over-all decrease in background, it was thought that it would be worthwhile to make some attempt to find out whether there were any indications of a large increase in O_3 concentration at the time of minimum. If there were an

[27] E. C. Y. Inn and Y. Tanaka, Absorption Coefficients of Ozone in the Ultraviolet and Visible Regions, J. Opt. Soc. Amer. 43, 870 (1953).

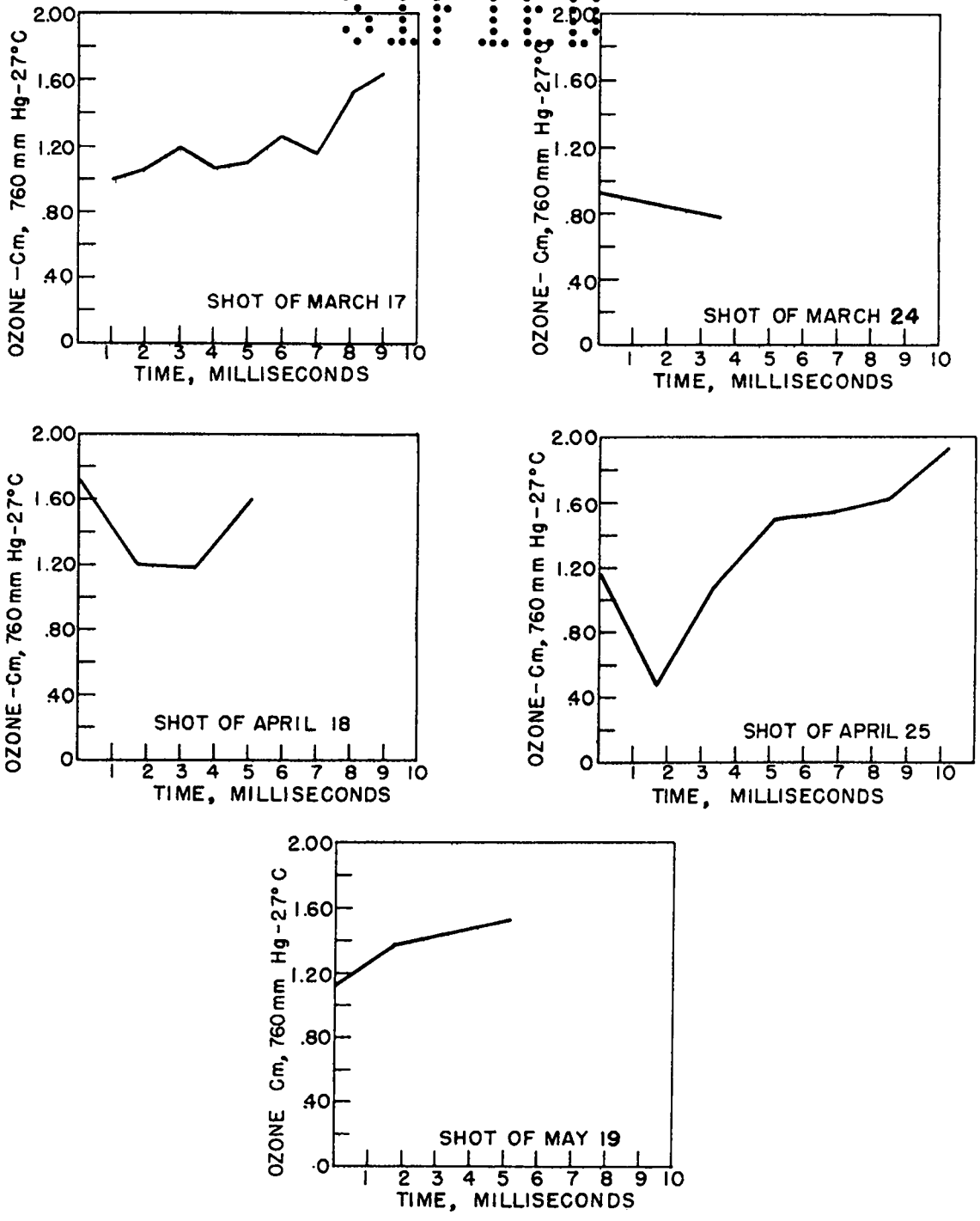

Fig. 25. Curves of O_3 content (cm) vs time. O_3 content is expressed as equivalent thickness of pure gas between spectrograph and bomb. (From NRL-4337)

increase in the O_3 content to about 10 equivalent centimeters during the minimum, this should be evident in the Chappuis region of 5500 to 6000 A. A careful examination of this region for all shots shows there is no pronounced structure difference between the first available spectrum and the spectrum during time of minimum. This may be seen by comparing Figs. 4 and 6, the latter corresponding to the time of the minimum. If these two tracings were superimposed they would cross in the region of interest, 5500 to 6000 A, but there is no pronounced difference between them. It seems likely that neither ozone nor a change in concentration of ozone plays an appreciable role in the formation of the minimum. The behavior of O_3 concentration as a function of time is probably similar to that of HNO_2.

6.3 OH

On some of the high speed spectra near the ultraviolet cutoff appear some sharp bands which sometimes can be partly resolved into fine lines. The wavelengths suggest that this absorption is due to OH formed by the dissociation of H_2O by secondary electrons or in other ways. The OH bands are best observed on spectra for the very smallest shots because the ultraviolet cutoff is shifted down to 2900 A and allows one to see a well defined recording of the 0-0 band of OH in absorption.

A total time spectrum from the first of these extremely small shots shows several interesting features. The space resolution that was possible showed the spectrum to be a dual one. In the center of the exposure corresponding to light from the central region of the

fireball, the spectrum is characteristic of the first maximum. For example, the low rotational temperature Schumann-Runge absorption bands are nicely delineated. However, at the edges of the same spectrum one sees the characteristic absorption of the high temperature Schumann-Runge bands which are not normally seen until the second maximum. From 3370 A on to higher wavelengths the edges of the spectra show the absorption spectrum characteristic of the second maximum, which includes structure due to AlO, FeO, Ba, Cu, Fe, and Al. At about 3700 A the entire fireball (center and edges of spectrum) appears to have a spectrum similar to that of the second maximum.

Apparently, in the region below 3700 A, the fireball had a dark center during the second maximum. The first maximum was recorded on the plate and the second maximum appeared at the edges of the slit but did not have sufficient intensity at the center to obliterate the already recorded first maximum spectrum, especially the low wavelengths. This general behavior is borne out by observations made with streak cameras which show that these peculiar small bombs appear to have a dark hole in the center at the very short second maximum.

Because of the low ultraviolet cutoff (2920 A) the 0-0 band of OH could be seen particularly well. An analysis[28] of the rotational intensity distribution in this band gives a rotational temperature of approximately 300°K in agreement with the rotational temperature which

[28] G. H. Dieke and H. M. Grosswhite, "The Ultraviolet Bands of OH," Johns Hopkins University Bumblebee Report No. 87, November 1948.

one finds from the distribution in the Schumann-Runge bands of the first maximum. Table 5 gives the wavelengths and recorded intensities of some of the lines of the 0-0 band and the 1-1 band.

TABLE 5

INTENSITIES OF SOME ABSORPTION LINES OF OH

Wavelengths, A	K	Background Densities	Line Densities	Background Minus Line Density
0-0 Band, R_1 Branch				
3072.03	1,1'	1.00	0.02	0.98
3070.35	2,2'	1.00	0.01	0.99
3068.75	3,3'	0.98	0.06	0.92
3067.30	4,4'	0.98	0.26	0.72
3065.98	5,5'	0.98	0.42	0.56
3064.49	6,6'	0.96	0.61	0.35
3064.19	7	0.96	0.74	0.22
3063.73	8	0.95	0.85	0.10
1-1 Band, Q Branch				
3134.58	1,1'	1.24	1.09	0.15
3136.17	2	1.24	1.08	0.16
3137.92	3,3'	1.24	1.12	0.12
3139.79	4	1.24	1.15	0.09
3141.91	5	1.24	1.18	0.06

6.4 N_2, N_2^+, and CN

Both N_2 and N_2^+ appear in emission in the Teller light. The N_2 bands clearly visible are the second positive group which requires 11 volts excitation energy. The first positive group which originates from the final state of the second positive group must also be expected.

There is considerable structure in the red of the high speed spectra of the Teller light but the resolution is not sufficient there to identify the structure definitively with the first negative group.

The N_2^+ bands appear both in emission in the Teller light and in absorption later on. The reason that N_2^+ is seen in absorption while the N_2 bands do not occur is simple. The N_2 absorption from the normal state occurs in the inaccessible ultraviolet. The near ultraviolet and visible bands occur between highly excited states and because of their short life (of the order of 10^{-8} sec) there is never a large enough concentration of molecules in this state. On the other hand, the N_2^+ state is stable, and a fair concentration of N_2^+ ions is produced by the gamma rays.

An exposure between 0.4 and 0.5 sec for the last shot of the 1953 series in Nevada showed at the lower wavelengths Schumann-Runge absorption due to O_2, and emission due to N_2, N_2^+, and CN. It is thought that this spectrum probably resulted from radiation originating near the periphery of the fireball. Table 6 gives the emission band wavelengths and the corresponding vibrational transitions identified for this shot. Emission lines from CN, N_2, and N_2^+ are also seen in total time spectra of the very small shots.

TABLE 6

OBSERVED N_2, N_2^+, AND CN EMISSION BANDS

N_2^+ Wavelength, A	N_2 Wavelength, A	CN Wavelength A
2563.9 (2-1)	3371.3 (0-0)	3585.9 (2-1)
3582.1 (1-0)	3576.9 (0-1)	3590.4 (1-0)
3884.3 (1-1)		3854.7 (3-3)
3914.4 (0-0)		3861.9 (2-2)
4651.8 (1-3)		3871.4 (1-1)
4709.2 (0-2)		

6.5 NO

NO is undoubtedly formed in the air ahead of the shock at a very early stage. The equilibrium concentration of NO is very high, e.g., at normal density and 4000° it is 8%, at 3000 or 6000° about 5%. Absorption by normal NO molecules lies in the inaccessible ultraviolet (about 2200 A), but when higher vibrational states are excited, the bands spread out into the visible, in a manner similar to the Schumann-Runge bands.[29] It is therefore hard to understand why the NO bands have not been observed. Hoerlin (private communication) has suggested that the NO spectrum has very little structure and is therefore very difficult to identify; this may be the explanation for the failure to detect NO bands in bomb spectra thus far. Moreover, NO may be the molecule chiefly responsible for the emission of air near the second maximum, and it may then be difficult to detect the absorption of the same

[29] See, e.g., R. Schmid, T. König and D. v. Farkas, Z. Physik 64, 84 (1930).

molecule in the cooler surrounding air. Altogether, the absence of NO is perhaps the greatest puzzle of the observed spectra.

6.6 Atomic Oxygen

The strong oxygen triplet at 7771.96, 7774.18 and 7775.40 A (3^5 S - 3^5 P) shows clearly in absorption. The lower state (3^5S) lies 9.11 volts above the ground state, but is the lowest state in the quintet system and therefore metastable. The lines of this triplet are quite definitely more diffuse than the surrounding atmospheric absorption lines. This may mean that when the O_2 molecule is dissociated the two atoms part with considerable kinetic energy so that the widening is due to Doppler effect.

7. CONCLUSIONS

An obvious expectation is that the spectrum must reflect the composition of the bomb, i.e., one must find in the spectrum the lines of all the elements contained in the bomb. This statement is neither strictly true nor would it be of great interest if it were true, since the composition of the bomb is already known. The spectra do reveal how the different materials are distributed in the fireball and at what stage they reach the outside where they can be detected. Not much is known about this distribution yet because most high dispersion spectra have neither time nor space resolution.

There seems to be a general relationship between the yield of the bomb and the structure of the spectrum. Small bombs show metallic

absorption well, whereas air absorption predominates in the larger bombs. Again, any general relationship is obscured by the lack of sufficient time and space resolution in high dispersion spectra, and also different regions of the spectra were often obtained for different shots.

Except perhaps for the very smallest bombs all the shots show distinctly different spectra for the first and second maxima. The spectra of the first maximum and a few milliseconds thereafter show mainly absorption by air and reaction products of the disturbed air preceding the shock front. At the time of the second maximum one sees absorption by a mixture of disturbed air and vaporized bomb constituents between the shock front and the fireball. The reaction products of air are less important and obscured by metallic absorption.

In the immediate vicinity of the fireball reactions take place which are often not similar to those familiar in laboratory experiments. These reaction products modify the absorption by air and affect how far we can see into the fireball. Particularly in the early absorption spectra one sees clearly bands due to NO_2, HNO_2, O_2, and OH, as well as excited O_2. Not much is known about their formation, though probably gamma radiation has a lot to do with it.

Some laboratory investigation is needed to find out whether such substances are formed in appreciable concentrations behind the shock front of a high velocity missile. Also more experiments are needed to measure the absorption coefficients of these substances at

high temperatures. Even small amounts of HNO_2 if formed behind a missile shock front might lead to a sizable amount of radiation because of the great width of the bands. Room temperature NO_2 has small absorption in the 6000 A region, but the possibility of a low-lying electronic state to which many NO_2 molecules may be raised at high temperatures may give rise to a much larger absorption coefficient in the 6000 A region for high temperature NO_2. On the important molecule NO, the bomb spectra have so far not given any information.

LOS ALAMOS AND NAVAL RESEARCH LABORATORY DOCUMENTS USED FOR THIS REPORT*

J. L Magee and J. O. Hirschfelder, Thermal Radiation Phenomena, Chpt. 4, LA-1020, August 1947.

G. H. Dieke, The Spectroscopy of Bomb Explosions, Los Alamos Scientific Laboratory Report LA-1329, August 29, 1952.

C. H. Duncan, Color Temperature of Weapons Exploded at Upshot-Knothole, Preliminary Report on Project 18.3, NRL Report 4356, April 1954.

J. A. Curcio, The Observed Variation with Time of the Amount of NO_2 Around Exploding Nuclear Weapons, Preliminary Report on Project 18.3, NRL Report 4322, February 1954.

J. A. Curcio, Spectrographic Observation of the Time Variation of O_3, HNO_2, and O_2 Generated by the Weapons Exploded at Upshot-Knothole, Preliminary Report on Project 18.3, NRL Report 4337, March 1954.

J. A. Curcio, Atlas Depicting Chronological Spectral History of the Shot of April 18, 1953, Preliminary Report on Project 18.3, NRL Report 4378.

J. H. Campbell and L. F. Drummeter, Jr., A Preliminary Survey of High Dispersion Spectrograms Obtained at Upshot-Knothole, Preliminary Report on Project 18.3, NRL Document RD 321.

J. A. Curcio, Atlas of High Dispersion Spectra Recorded at Buster-Jangle, Preliminary Report on Project 10.9, NRL Report 4386, June 1954.

J. A. Curcio, Atlas of High Dispersion Spectra Recorded at Greenhouse, Auxiliary Report on Project NRLH, NRL Report 4434, September 1954.

*The Naval Research Laboratory reports listed here are preliminary reports which are not available for distribution. The information will appear in formal weapon test reports to be issued at a later date.